國立臺灣大學醫學院暨工學院醫學工程學研究所

碩士論文

Institute of Biomedical Engineering

National Taiwan University

Master Thesis

利用擴散頻譜磁振造影神經纖維成像分析精神分裂症白質完整度：手動與自動化模板模式之比較

Diffusion spectrum imaging tractography analysis of white matter integrity in patients with schizophrenia: Comparison between manual approach and template-based automatic approach

何致煒

Jhih-Wei He

指導教授：曾文毅 醫師、博士、林發暄 博士

Advisor: Wen-Yih Isaac Tseng, M.D., Ph.D., Fa-Hsuan Lin, Ph.D.

中華民國 100 年 7 月

July, 2011

誌謝

在生醫影像核心實驗室兩年的學習過程，隨著論文的付梓，即將劃上句點。感謝指導老師曾文毅教授兩年間的指導，無時不給我機會，同時也給我許多考驗。我相信老師兩年的教導，我將受用一輩子。感謝指導老師林發暄教授給予我許多生活觀念上的幫助以及解決事物的新觀點。

感謝口試委員陳中明教授、王兆麟教授、黃宗正醫師提點我許多研究上待解決的問題。感謝精神科胡海國醫師、劉智民醫師、劉震鐘醫師開會時給予之建議。感謝腫醫所吳文超教授益師益友的討論，心理所周泰立教授、葉怡玉教授平時的關心。

謝謝曜嘉、筱瑾、柏諺給我同儕間的刺激以及苦中作樂的美麗時光。我們的足跡踏遍了醫學院每個留有青春氣息的角落，在空靜的山徑中攤坐戲謔大笑而後焚燃胸腔。也特別謝謝曜嘉在口試期間的幫忙及陪伴。

謝謝香彌子博士給予我許多支持，每次的談話都很有啟發性。謝謝伃君學姐神經纖維束的經驗指導，謝謝泳欽學長的模板讓我有機會發揮。謝謝國強學長實驗時的教導，謝謝素君學姐幫忙收案。謝謝立威、芳誠、文揚三位學長撥冗寫信回覆我的問題。謝謝麗婷學姐教我使用許多軟體及研究方法，謝謝品妤學姐幫忙我的統計疑惑。謝謝振豪醫師以我為鏡，讓我知道自己的研究程序是否適當。謝謝政達醫師同我做施測間信度，謝謝志紳時常幫我修改英文。

謝謝冠良、小火車、懌華、懿桓、欣婕、曉嵐、蘊生等實驗室夥伴，以及幫忙我很多的醫工所閔如助教。謝謝周泰立教授實驗室的兩年來一起合作收案的利霙、姝慧、品臻等同學們、精神科宣惟以及放射師學長姐們的幫忙。謝謝所有參與收案的受試者，因為有你們時間和精神上的付出，我們才能有些許的貢獻。

謝謝好友宜憲、奎含、祖濬、朕宇、同謙、振益、秋秋、淑如、皮卡、小白、聖銘、津儷、令明、維謙平常的關懷。最後誠摯地感謝生養育我的父母何俊傑先生、劉麗珍女士一直以來的支持，你們永遠是天上最耀眼的兩顆星。

中文摘要

精神分裂症是現代社會中影響身心靈、經濟很大的疾病，在台灣的盛行率約為 0.3 至 1%。患者主要有幻覺、妄想、怪異行為等臨床表現。長期下來，也會有合併認知功能障礙以及造成情緒表達上的障礙。目前現有的研究讓我們了解到精神分裂症的病因之一可能是大腦各灰質區塊間聯繫出現阻礙，因此研究白質的神經完整性是當今的重要課題。再者，許多研究說明額葉眼眶面皮質與負向情緒以及焦慮的抑制有關，而這也是精神分裂症患者主要症狀。因此我們選定了下述三組連接至額葉眼眶面皮質的神經束來分析其完整性：兩側的前丘腦放射、兩側的鉤束以及胼胝體膝。此外，探討症狀輕重與神經完整性之關連亦為本研究之目標。

本研究共招募了二十位長期精神分裂症患者與二十位年齡性別相對應之對照組，每位受試者均接受擴散頻譜磁振造影以及 T2 權重影像二種磁振影像掃描，患者並於掃描前後門診接受活性與負性症狀量表之評估。首先使用手動模式神經纖維成像術來重建上述三組神經影像，並計算其總擴散不等向性。接著，比較病人組與對照組間之差異，並分析病人組中，總擴散不等向性與活性與負性症狀量表分數之相關。

組間結果顯示，相較於對照組，病人組除右側前丘腦放射之總擴散不等向性下降不夠顯著外，其餘神經束均有下降至顯著差異。總擴散不等向性與活性與負性症狀量表分數之相關結果顯示，胼胝體膝之總擴散不等向性與焦慮/憂鬱因子之分數有負相關。

此外，本研究另一目的為使用自動化模板模式來重現手動模式之結果。本模式中，病人組相較於對照組之總擴散不等向性均有下降但未達顯著。但由於擴散頻譜影像之標準化，我們可以得到等長的總擴散不等向性描繪圖，進而了解平均總擴散不等向性在解剖位置上高低值之分布並進行組間比較。結果顯示病人組的胼胝體膝與左側上縱束交錯位置之總擴散不等向性比對照組高。此外，前丘腦放射在丘腦位置之總擴散不等向性，對照組有左大於右的側化現象，而病人組沒有發現此現象。

在兩模式比較中，自動化模板模式所得到之總擴散不等向性與手動模式有高度正相關，且自動化模板模式所得到之總擴散不等向性描繪圖可與手動模式之結果互相呼應。

本研究顯現了擴散頻譜磁振造影與神經纖維成像術在精神分裂症中探討活體白質完整性的方便性，也讓我們對於精神分裂症的病理有更深一層的體認。另一方面，自動化模板模式中總擴散不等向性描繪圖的分析，也讓我們從整條神經束總擴散不等向性進而深入分析不同解剖位置。

未來手動模式與自動化模板模式將會相輔相成，融合個別特點以補足彼此之缺陷，以辟找到精神分裂症或其他疾病在神經影像診斷學上的生物標記。

關鍵字：精神分裂症、額葉眼眶面皮質、前丘腦放射、鉤束、胼胝體膝、活性與負性症狀量表、擴散頻譜磁振造影、總擴散不等向性、總擴散不等向性描繪圖

Abstract

Schizophrenia is a high-impact mental disorder that affects approximately 0.3~1% of the population in Taiwan, with ravaging effects on both psychological and economical resources. This serious mental illness not only affects our cognition but also contributes to chronic emotional problems. Disturbed communication of white matter within the brain region may be the possible pathology of schizophrenia, which was mentioned previously. Therefore, it's important to investigate the white matter's integrity. Also, the orbitofontal cortex (OFC) was linked to negative emotions and anxiety, which were the symptoms of schzophrenia. There are three white matter tracts which connected to the OFC chosen to be studied in the investigation of the difference between patients with schizophrenia and normal control patients in our research: bilateral anterior thalamic radiation (ATR), bilateral uncinate fasciculus (UF) and genu.

We recruited 20 patients with chronic schizophrenia and age- and gender-matched healthy controls to acquire diffusion spectrum images and T2-weighted structure images. The patients' PANSS scores were measured in outpatients one week before the MRI scan or one week after the scan. The first, tractogrphy of ATR, UF and genu was rebuilt in a manual approach, and the general fractional anisotropy (GFA) was calculated. Then, we compared the difference between two groups and analyzed the correlation between GFA values and PANSS scores.

In the results, the GFA values were significantly reduced in all tracts except the right ATR in schizophrenia. And there was a negative correlation between GFA values in the genu of a factor of 5 (anxiety/depression).

Moreover, we used an automatic template-based approach to compare results to

the manual approach. In this approach, we found that there was a trend that all GFA values of tracts in schizophrenia were lower than normal controls' even though it was not significant. But we could compare the profiles between groups because the lengths of the GFA profiles were the same after normalization. We found the mean GFA value in schizophrenia was higher in the genu in the intersection with left superior longitudinal fasciculus (SLF). Also, there was a left-right asymmetry in thalamus in normal controls.

There was a significant positive correlation of GFA values between these two approaches. These two approaches were auxiliary to each other because they possessed different traits and could be explained together.

Our findings showed the usefulness of applying DSI and tractography to investigate white matter fiber tracts in vivo in schizophrenia, and thus extended our understanding of the pathophysiology of this disease. Also, we could investigate the different parts of the GFA profile by the automatic template-based approach.

In the future, we will combine these two approaches in order to find the neuroimage biomarker of schizophrenia or other diseases.

Key words: schizophrenia, orbitofrontal cortex, anterior thalaic radiation, uncinate fasciculus, genu, PANSS, diffusion spectrum imaging, general fractional anisotropy, GFA profile

Contents

Lists of Figures

Lists of Tables

Chapter 1

Introduction

1.1. Schizophrenia

Schizophrenia is a high-impact mental disorder that affects approximately 1% of the general population (24 million people worldwide), and 0.3~1% of the population in Taiwan, with ravaging effects on both psychological and economic resources. This serious mental illness not only affects our cognition, but also contributes to chronic problems of emotion.

Synaptic pathology leading to aberrant cortical circuitry has been well

documented in neuropathological studies (Harrison & Weinberger, 2005). And, disturbed communication of white matter within the brain region which is mentioned by Wernicke (1906) as the “disconnection hypothesis ”may be the possible pathology of schizophrenia (Friston, 1998). Also, some studies, both in vivo and post-mortem, have shown the difference of white matter volume, fiber number, or density between schizophrenia patients and normal controls due to demyelination, reduced oligodendrocyte numbers, or integrity (Segal, Koschnick, Slegers, & Hof, 2007).

Therefore, the investigation of the integrity of white matter fiber tracts connecting these brain regions is a critical issue of the study in schizophrenia.

1.2. Orbitofrontal cortex and emotion

The orbitofrontal cortex (OFC) which consists of Brodmann areas 10, 11, and 47 is a part of the prefrontal cortex. It receives information from the ventral or object processing visual stream, and taste, olfactory, and somatosensory inputs (Rolls, 2004) (Figure 1). It is a nexus for sensory integration, the modulation of autonomic reactions, and participation in learning, prediction and decision making for emotional and reward-related behaviors. In a rhesus monkey study in 1972, it was found that damage to the caudal orbitofrontal cortex lead to emotional changes, and a reduced

tendency to reject foods (Butter & Snyder, 1972). It was also involved in representing and learning about the reinforcers that elicit emotions and conscious feelings such as touch (Francis, et al., 1999). Also, while doing the Iowa gambling task with concurrent measurements of galvanic skin responses, or skin conduction responses; patients with OFC dysfunction never had a “stress” reaction to impending punishment when they made a wrong choice. This result revealed that patients with OFC dysfunction don’t have emotional distinction between choices with good or bad future outcomes (Bechara, Tranel, Damasio, & Damasio, 1996).

Because of its functions in emotions and rewards, the OFC was considered to be a part of the limbic system and it also offered important insights into emotional disorders such as depression (Kringelbach, 2005). In an imaging study by magnetic resonance imaging, the cortical volumes of the bilateral orbital gyri were found significantly reduced in patients with schizophrenia compared with those in healthy subjects (Takayanagi, et al., 2010).

That means some psychopathological correlation with the OFC was found in patients with schizophrenia. Furthermore, the white matter connecting the OFC with other brain regions was worth investigating. Therefore, investigating the integrity of white matter tracts between two brain regions was important to understand this mental disease. Also, the study of abnormalities in intra- and inter-hemispheric

pathways has obtained less attention in neuroimaging study, even though the occurrence of symptoms of schizophrenia has mentioned in disease involving the white matter (Walterfang, Wood, Velakoulis, & Pantelis, 2006).

1.3. Genu, Anterior thalamic radiation and Uncinate fasciculus

In schizophrenia, the brain's grey matter areas where change commonly happens are the prefrontal cortex including OFC (Jones, et al., 2006) and the temporal cortex (Rosenberger, et al., 2008). There were three white matter tracts chosen to be investigated in the difference between patients with schizophrenia and normal controls in our research. All of them connect the orbitofrontal cortex and other brain regions. These three tracts are mentioned as following: The first one is the genu, which is the anterior part of the corpus callosum connecting the left and right prefrontal cortex, is a commissural fiber. The second one is the anterior thalamic radiation (ATR), which projects from the anterior nuclei of thalamus to the prefrontal cortex and is a projection fiber. The third one is the uncinate fasciculus (UF), which connects the prefrontal and temporal cortex of each brain hemisphere and is an association fiber (Figure 2). The details of these three fiber tracts are mentioned as following.

1.3.1. Genu

Additional evidence regarding interhemispheric connectivity abnormalities comes from electrophysiological studies demonstrating differences in latency and coherence between patients with schizophrenia and healthy controls (Norman, et al., 1997). Some findings are compatible with previous reports of decreased volume of the genu, which is a part of the corpus callosum connecting the left and right OFC, in schizophrenia (Hulshoff Pol, et al., 2004). Furthermore, in previous diffusion tensor imaging studies, Kubicki (2008) found reduced fractional anisotropy in the prefrontal part of the corpus callosum, which connects the entire frontal cortex, by using the ROI approach and mapping an already existing tractography based atlas onto their DTI data. And also, Shergill (2007), who used the voxel-based approach, has demonstrated reduced fractional anisotropy in the genu. Therefore, to understand the integrity of the genu by the tractography method is important even now.

1.3.2. Anterior thalamic radiation

The thalamus plays an important role in the conformity of information as it moves from region to region within the brain. A disruption of that information may lead to some of the essential symptoms of schizophrenia. Evidence from many studies has

implicated thalamic dysfunction in schizophrenia. In postmortem studies, reduced numbers and volumes of mediodorsal and anterior thalamic neurons were exposed in patients with schizophrenia (Byne, Hazlett, Buchsbaum, & Kemether, 2009).

Through in vivo studies using magnetic resonance imaging, Konick and Friedman (2001) have demonstrated reduced volumes of thalamus in schizophrenia, as well as shape deformations suggesting changes in those thalamic regions that are most densely connected to the regions of the brain responsible for executive function and sensory integration such as the prefrontal cortex (Konick & Friedman, 2001). These changes seem to correlate with clinical symptoms.

Also, the thalamus is the origin for several perplexed, overlapping networks that extend from the thalamic nuclei to the cortex. Evidence is emerging that changes in the thalamic nucleus of these networks, such as the cortico-thalamic circuit, are influenced by changes at other brain regions along the chain; this suggests that schizophrenia might be a disease of disrupted thalamocortical neural networks (Lopez-Bendito & Molnar, 2003).

Also, the anterior thalamic radiation is a kind of projection fiber formed by white matter interconnecting, via the anterior limb of the internal capsule, the anterior and medial thalamic nuclei, and the frontal cortex. The activity of striatum and thalamus is modulated by the prefrontal cortex, and this process is understood to be key to the

appreciation of rewards, emotional processing, and mood (Sussmann, et al., 2009)

Therefore, the integrity of the ATR connection between the thalamus and the OFC is a critical issue worth figuring out.

1.3.3. Uncinate fasciculus

The uncinate fasciculus (UF), which is the largest white matter tract of the fronto-temporal connections, is a ventral limbic pathway that connects the ventral, media, and orbital parts of the frontal cortex and temporal lobe areas, such as the inferior temporal cortex. It connects brain regions involved in sound and object recognition (superior and inferior temporal gyri) and recognition memory (entorhinal, perirhinal and parahippocampal cortices) with orbitofrontal areas implicated in emotion, inhibition, and self-regulation (Price, et al., 2008). Thus, the UF is a very important tract in the interaction between cognition and emotion (Barbas, 2000). It is also important to study the integrity of this tract.

1.4. Fiber integrity and diffusion

The physical phenomenon that molecules in liquid or gas diffuse randomly is called Brownian motion. If we want to detect the diffusion pattern of molecules, we have to orient the molecules and trace their position variation per unit time. There are several ways to trace the molecules such as the radioactive tracer measurement, neutron scattering spectroscopy, and diffusion MRI. The first two methods are not as necessary to apply to the human body due to invasive agents, even in the millimeter and angstrom range, can be measured. However, the micrometer range, which is the most suitable range of neuron axons, can be detected using the diffusion MRI technique, and water molecules as a natural agent in the body are non-invasive (Le Bihan, 1995).

The molecules in a certain magnetic field spin in a certain frequency called the Lamor Frequency. And after the molecules diffuse over a certain time, their position will change and suffer different magnetic magnitudes, and accumulate the precession phases. This phenomenon will cause the signal decay. In 1950, Hahn first found that the signal of a spin echo would be attenuated by diffusion (Hahn, 1950). In 1956, Torrey (1956) mentioned the relationship between signal decay and the diffusion effect, and added a diffusion term into the Bloch equations (Torrey, 1956).

Later, the bipolar pulsed gradient spin echo sequence (PGSE) was proposed in

which two diffusion gradients were implemented between 90 and 180 degree RF pulse, 180 degree RF pulse and echo (Stejskal, tanner 1964). It explained the diffusion effect in a steady magnetic gradient field (Figure 3).

In 1984, Wesbey purposed the principle of diffusion MRI which combined diffusion MR techniques and the concept of detecting the diffusion of water molecules (Wesbey, Moseley, & Ehman, 1984). The signal spin echo of water molecules would be attenuated due to the phenomenon of diffusion and perfusion, for the reason that diffusion MRI applied in vivo is possible (Le Bihan, et al., 1986). Later, ischemia in cat brains was detected by diffusion MRI, and the attenuation of the diffusion signal reflected the early stage of ischemia in the brain (Moseley, et al., 1990). It was the first study in organisms, and the early stages of hemorrhagic stroke could also be detected.

Because the velocity of diffusion was small, the large diffusion gradients were adjusted to accumulate the effective phase. Therefore, we can use the situation of water diffusion in vivo to determine the integrity of the tissues.

1.5. Diffusion Spectrum Image and tractography

One of the ways to investigate the integrity of white matter tracts is diffusion tensor imaging (DTI) (Basser, Mattiello, & LeBihan, 1994), which has used in the research of neuroimaging for many years. The integrity of white matter can be measured quantitatively from the eigenvalues of a diffusion tensor by DTI. One of the indexes used widely to measure the situation of water diffusion is fractional anisotropy (FA), and it is derived from the three eigenvalues of a diffusion tensor. The formula of FA is (the standard deviation of the three eigenvalues)/ (the root mean square of the three eigenvalues). If the first eigenvalue is one and other two are zero, the value of FA will be one, and that represents that the water diffusion is extremely anisotropic. If the three eigenvalues are all the same, the value of FA will be zero, and that represents that the water diffusion is isotropic. Hence, a higher value of FA reflects a higher fiber density, larger axonal diameter, and higher level of consistent myelination of the brain's white matter (Scholz, Klein, Behrens, & Johansen-Berg, 2009) (figure 4).

By using DTI, there are three approaches to study the brain's white matter integrity, which are the voxal-based approach, the ROI approach, and the tractography-based approach (Kanaan, et al., 2006). The tractography-based approach allows us to investigate the integrity along a bundle of white matter tracts, so it is the most suitable one to study the integrity of white matter tracts between two

brain regions.

However, the fiber tracts of the human brain are intricate. That means the fiber tracts may be crossing or kissing to others because the white matter is an interweaving web structure. And this problem can't be solved by using DTI, because it is reconstructed by only a single tensor in a voxel. In order to solve this troublesome problem, a high angular resolution diffusion method called diffusion spectrum imaging (DSI) (Wedeen, Hagmann, Tseng, Reese, & Weisskoff, 2005), which helps to investigate the divergence of water diffusion within a voxel, is used in our research.

DSI is a MRI technique which records the displacement in more than one hundred directions (depending on the No. of diffusion gradients) of every water molecule at each voxel. And it provides the information of the probability distribution of water molecular displacement at each voxel. Then the reconstructed tractography based on DSI can solve the problem of crossing or missing fibers at each voxel (figure 5).

After doing tractography, we want to compare the property of each tract between patients in schizophrenia and normal controls. Here, DSI provides us a diffusion index named general fractional anisotropy (GFA) which is computed for each individual voxel based on the shape of the original ODF. The formula of deriving the value of GFA is (the standard deviation of ODF)/(the root mean square of ODF) (Tuch, 2004).

Like fractional anisotropy (FA) of DTI, GFA also stands for the integrity of the white matter fiber tracts (Liu, et al., 2010).

To better understand the anatomical changes in schizophrenia, we used diffusion spectrum imaging (DSI) with the tractography approach to investigate the differences in structural connectivity of the tracts schizophrenia patients and normal controls.

1.6. PANSS factors

The PANSS or the Positive and Negative Syndrome Scale is a medical scale used for measuring the severity of symptoms of patients with schizophrenia. It was published in 1987 by Stanley Kay, Lewis Opler, and Abraham Fiszbein. It is widely used in the study of antipsychotic therapy (Kay, Fiszbein, & Opler, 1987). The positive symptoms and the negative symptoms can be detected effectively by this medical scale.

In 1995, the Chinese version was established by Hu's group in NTU Hospital. They grouped the sub-items into four factors as Positive (seven sub-items), Negative (seven sub-items), General (sixteen sub-items), and others (three sub-items).

And in 1990, Kay and Sevy (1994) regrouped the thirty sub-items into five independent factors by factors analysis, which were Negative symptoms (seven

sub-items), Positive symptoms (eight sub-items), Disorganized thought (seven sub-items), Uncontrolled hostility/excitement (four sub-items), and Anxiety/depression (four sub-items) (Kay & Sevy, 1990).

The highest score of each sub-item is seven, which means extreme severity. And the lowest score of each sub-item is one, which means symptom absent. The total score is 231, and requires 45 to 50 minutes for a brief interview by trained clinical psychiatrists.

1.7. A new template-based approach

In the neuroimaging research field, image registration is an important issue. Because a good template can make the comparison more objectively by normalizing the source image (individual brain) to the target image (the template). However, the realigning of the fiber orientation of the diffusion MRI data in the same way among different brains is not readily applicable.

There was a two step method to reorienting the fiber tracts on DTI datasets: the first, to register the DTI dataset (image space) by the 3D registration method; the second, to reorient the diffusion tensor of the dataset according to the “preservation of principal direction” rule (Alexander, Pierpaoli, Basser, & Gee, 2001). However, the

method can't be applied to high angular resolution diffuion imaging (HARDI) sampling schemes such as DSI because there was no tensor used. Therefore, one senior member of our lab developed a method for DSI dataset registration by using the 6D Large Deformation Diffeomorphic Metric Mapping (LDDMM) algorithm (Beg, Miller, Trouve, & Younes, 2005; Hsu et al.,2009) since the DSI dataset is essentially in a 3D image space and 3D q-space.

The LDDMM algorithm models the image registation as fluid mechanics where the target image 'flows' to match the source image (the template). And the variable velocity fields are calculated seperately and iteratively at each time point such that the energy function is minimized. The LDDMM algorithm provides a minimum path for deformation between target and template images. To save time, we extended the concept metioned by Ashburner (Ashburner, 2007) who had used ony single constant velocity fields to encode the whole path of transformation instead of Beg's original method, and used a constant acceleration field to encode the variable velocity fields (Hsu et al.,2009).

Performing the tansformation on the image space and the q-space simumultaneously by 6D LDDMM can prevent a problem in which fiber orientation can be sheared if we get a local rotation matrix from image space first, and then apply it to the q-space (Hsu et al., 2010).

In the template-based automatic approach, we draw the tractography on a DSI template, and normalize all individual DSI brains to the template. Then we sample the tractography which is drawn on the template to the normalized individual brain, calculate the GFA values, and also compare the GFA values between these two groups.

One advantage of the template-based automatic approach is saving time, because we only draw tractography once on the DSI template brain and then sample it with other individual DSI brains which are normalized to the template. Another advantage is that the tractography of one white matter tract will be the same in shapes, tract numbers, and length over every individual DSI brain. That allows us to compare the integrity of white matter in a normalized brain.

1.8. Manual approach as a reference method

In this study, we have two kinds of tractography approaches. One is the manual approach, and another one is the template-based automatic approach. In the manual approach, we do the tractography on every individual DSI brain, calculate the GFA values, and compare the GFA values between two groups (patients with schizophrenia and normal controls).

1.9. The goal of this thesis

Therefore, the first aim of this thesis is to compare the GFA values of these fiber tracts (bilateral ATR, bilateral UF, and genu) between patients with schizophrenia and normal controls in the manual approach. We want to investigate if the integrity of these fiber tracts is different between the patients with schizophrenia and the normal controls. Furthermore, the asymmetry patterns of ATR and UF of each group is also analyzed.

The second aim of this thesis is to investigate the correlation between the GFA values of these patients' fiber tracts and their PANSS scores. That means the relationship of the severity of the phenotype and integrity of the anatomical structure will be analyzed.

The third aim of this thesis is to compare the result of the fast automatic template-base tractography approach to the result of manual tractography approach. We want to see if the result is the same in both approaches. If it is, we could use the automatic template-based approach to do less time consuming research.

Chapter 2

Methods

2.1. Subjects

Between July 2009 and July 2010, we recruited 20 patients with chronic schizophrenia including 10 males and 10 females who were diagnosed according to the DSM-IV diagnostic criteria by qualified psychiatrists at the National Taiwan University Hospital. Exclusion criteria included the presence of DSM-IV Axis I diagnoses of other disorders such as bipolar disorder, history of any substance dependence or history of clinically significant head trauma. Their average age is 28 ±

7.6 years, and their mean education year is 13.4 ± 2.11 years. Only one of them was left handed and the other 19 were right handed, according to the Edinburgh Handedness Inventory. Nineteen of the patients' PANSS scores were measured one week before the MRI scan by clinical psychiatrists in outpatients, or one week after the scan.

We also recruited 20 age- and gender-matched healthy controls from the post on the internet. Their average age is 27.9 ± 7.52 years, and their mean education year is 16.28 ± 1.78 years. All of them are right handed and free of the DSM-IV diagnoses of schizophrenia and other DSM-IV Axis I diagnoses of other disorders, and were excluded for neurological diseases, history of any substance dependence, or history of clinically significant head trauma.

Written informed consent was obtained from all individual participants, and all of the research procedures and ethical guidelines were followed in accordance with the Institutional Review Board (IRB) of the National Taiwan University Hospital (Table1).

2.2. DSI MRI acquisition

All individuals, including the 20 patients with schizophrenia and the 20 healthy controls for comparison, were scanned on a 3-Tesla Magnetic Resonance Imaging system (Siemens, Erlangen, Germany) and the whole brain was covered on this system with a standard 32-channel head coil used as both an RF transmitter and signal receiver in the National Taiwan University Hospital.

T1-weighted, T2-weighted structure images, and Diffusion Spectrum Images were acquired with the same orientation slice and the same scan range. The slice orientation was stipulated parallel to the line which connected the anterior commissure and posterior commissure (AC-PC line), and the scan range is from the vertex to the inferior tip of the cerebellum.

In order to get a reference image of anatomy, a magnetization-prepared rapid gradient echo (MPRAGE) sequence was used to acquire a whole brain high-resolution T1-weighted MR image in a coronal view. The sequence parameters were TR/TE = 2000ms/2.98ms, image matrix size = 192 x 256, spatial resolution = 1 x 1 mm^2, field of view (FOV) = 192 × 256 mm^2 and slice thickness = 1 mm without gap. Total scan time was 3 minutes and 36 seconds.

Our T2-weighted structure images were acquired using a turbo spin echo sequence. The sequence parameters were TR/TE = 9430ms/101ms, image matrix

size = 256 x 256, spatial resolution = 0.97 x 0.97 mm^2, field of view (FOV) = 248 × 248 mm^2 and slice thickness = 3 mm without gap. Total scan time was 2 minutes and 14 seconds.

Our DSI images were acquired using a twice-refocused balanced echo diffusion echo planar imaging (EPI) sequence and the sequence could reduce the image distortion resulted from field gradient eddy currents. The following scan criteria were used: TR/TE = 9600/130 ms, image matrix size = 80 x 80, spatial resolution = 2.5 x 2.5 mm^2, field of view (FOV) = 200 × 200 mm^2 and slice thickness = 2.5 mm without gap. The diffusion weighting value (b-value) was set from 0 to maximum 4000 s/mm^2 along 102 diffusion encoding gradient directions. And all 102 signals acquired from the diffusion encoding gradient were sampled to an isotropic 3D q-space on grid points with $|q| \leqq 3$. The spatial modulation was $q=\gamma g\delta/2\pi$, in which γ is the proton gyromagnetic ratio, g is the diffusion-encoding gradient and δ is the diffusion gradient duration (Kuo, et al., 2008). Total scan time was 16 minutes and 29 seconds (Table 2).

Because the orbitofrontal cortex is very close to the air-filled sinuses, imaging the human OFC by MRI is a challenge. This means that when we use EPI at high field strength B_0 for DSI scanning, signal dropout and susceptibility artifacts are common phenomena. To solve this problem, we not only did automatic shimming before the DSI scan, but also did field mapping estimations of 10 MR scans having different echo

times from 27ms~36ms. But we set the same matrix size and FOV of the field maps as those used in the DSI dataset. In an EPI scan, it's advisable to do correction for the effect of field inhomogeneity to lower image distortion. The difference of phase between the acquired images is due to the different precession frequencies, which are related to the field map via a linear relation (Funai, Fessler, Yeo, Olafsson, & Noll, 2008; Hsu, Hsu, & Tseng, 2009).

Because the echo signal S (q) and diffusion probability density function P(r) were a Fourier pair, the diffusion probability density function P(r) was obtained from the echo signal S (q) which was sampled with the 3D q-space by a Fourier transformation. To obtain PDF, the whole data in the q-space which was applied to a Hanning filter of 17 in width was transformed by the 3D Fourier transformation method. (Callaghan, Coy, Macgowan, Packer, & Zelaya, 1991). And, the orientation distribution function (ODF) was calculated by taking the second moment of P(r) along each radial direction (Wedeen, et al., 2005). To find out the fiber orientations at each voxel, we used an iterative way to decompose the ODF into several partial Gaussian ODFs corresponding to the primary orientations at each voxel (Yeh et al., 2008) (Figure 6).

In present research, we decomposed the ODF into 362 directions in accordance with the vertices of a 6-fold regularly tessellated dodecahedron projected onto the sphere. Afterwards, the individual intravoxel fiber directions including the primary fiber

orientation were decided by decomposing the original ODF into 362 constitutional parts which were used for tractography construction.

Then, to quantify the structural connectivity, the generalized fractional anisotropy (GFA) of each voxel was computed according to the shape of the original ODF. It quantified the directionality of the diffusion on a scale from zero (when the diffusion was totally random) to one (when the diffusion was along one direction only).

Later, the tractography was reconstructed using a streamline-based algorithm adapted for DSI data by our in-house software DSI studio and the targeted tracts (genu, ATR and UF) were selected by placing specific regions-of-interest. Finally, the GFA was projected onto a single mean path of the tracts by mean path analysis.

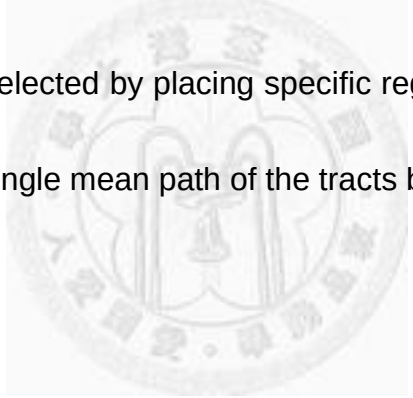

2.3. DSI tractography, tract-specific analysis (manual approach)

Before ROI selecting, we performed co-registration, which is a linear transformation between the null images of DSI (b_0) of each individual participant's brain and their T2 weighted image by a 3D affine transformation matrix. And also, we performed normalization, which is a non-linear transformation from the T2 weighted image of each individual participant's brain to the Montreal Neurobiology Institute (MNI) T2 weighted image template. Then, we got a deformation matrix in order to do

inverse transformation from the coordinates of the regions of interest (ROIs) defined in the MNI template to each individual participant's brain. The processes of coregistration, normalization, and deformation matrix calculating were all performed by SPM5 (Wellcome Department of Imaging Neuroscience, London, UK) (Figure 7).

For ROI selecting, we used MARINA (Bender Institute of Neuroimaging, University of Giessen, Germany) to define cortical regions as ROIs on the Montreal Neurobiology Institute (MNI) T2 image template (ICBM-152). For bilateral ATR, the ipsilateral orbitofrontal lobe and thalamus were selected for two ROIs. For each UF, the ipslateral orbitofrontal lobe and Superior temporal and medial gyrus of the temporal lobe were selected as two ROIs. For the genu, the bilateral orbitofrontal lobe was selected as an ROI. Therefore, we could transform the ROIs to each individual brain though the deformation matrix that was mentioned above.

After the ROIs were transformed to each individual brain, tractography was reconstructed using a streamline-based fiber tracking algorithm adapted for DSI data based on the resolved fiber vector fields by our in-house software DSI studio (DSI Studio: http://dsi-studio.labsolver.org) and the targeted tracts (genu, ATR and UF) were selected by placing specific ROIs. Furthermore, we set whole brain seed and GFA value thresholds of 0.1 to process the tractography.

At each seed voxel, the next step proceeding orientation could be decided by the

angular deviation between the major orientation within this seed voxel and all of the fiber orientations of the eight voxels which were near this seed voxel, and the most coincident orientation, which was used to choose the minimum angular deviation. For the ATR, UF, and genu, the angle thresholds were 30°, 45°, and 35°, respectively. The seed point was moving with a proceeding length of 1.24 mm or one-half voxel for every step along the most coincident orientation, and then a new starting point was obtained. If the angle deviation was higher than the angular threshold we chose, the tracking would be stopped. And also, we set the track lengths between 20mm and 200mm, and the tract number of 200 for each targeted fiber tract to avoid incorrect tractography (Figure 8).

After the tractography was reconstructed, we confirmed whether the entire trajectory was consistent with other established anatomical landmarks shown in the atlases of tractography used as references (Mori et al., 2005).

Later, we used mean path algorithm which was developed in Matlab (The Mathworks, Natick, MA, USA) by a senior member of our lab (Chiang et al., 2007) to do tract-specific analysis. In this algorithm, we built an initial ball of radius 5.5mm to cover the tract bundle, and decided on an orientation for further calculation. There was a plane which intersected with the fibers established in the ball to calculate the mean direction of the tracts. Here, we set Std. of Directions of Fibers to 0.25 as a stop

criterion in order to avoid the orientations of the fiber tracts dispersing too much. After the geometric mean of the coordinates on which the fiber tracts intersected on the target plane were calculated at each step, all of the fiber tracts intersecting on the target plane were considered to have the same coordinates as the geometric mean. And the plane moved and calculated the geometric mean of the coordinates step by step (1.22mm) along the orientation we set until attaining our stop criterion.

Here, we had another parameter named “fiber ratio for terminaton”, and this ratio was defined as [the number of fibers on the crossing plane (peripheral branches)]/ [the number of fibers on the densest crossing plane (the trunk)]. In our research, the ratio is set to 0.6 in order to reduce the bias due to the variance of peripheral banches which might be thought to own lower GFA values than the trunk. Therefore, if the fiber ratio for terminaton was below 0.6, the calculation of the mean path would be terminated automatically. Finally, a profile of GFA values along the tract bundle and mean GFA values were obtained (Figure 9).

In the manual approach, we do the tractography on every individual DSI brain, calculate the GFA values, and compare the GFA values between two groups (patients with schizophrenia and normal controls).

2.4. Template approach: Spatial normalization, template tractography

In the template-based automatic approach, we made a template for DSI data normalization. The template we used was made from 20 healthy subjects (25.2 ± 4.5) including 12 males (26.3 ± 3.3) and 8 females (23.5 ± 5.7), and all subjects were scanned using a standard 32-channel head coil on a 3T MRI scanner (Siemens, Tim Trio). Their DSI datasets of 203 points in q-space with b-values up to 4500 s/mm^2 were acquired. The following scan criteria were used: TR/TE = 9600/130 ms, image matrix size = 80 x 80 x 56, spatial resolution = 2.5 x 2.5 mm^2, field of view (FOV) = 200 × 200 mm^2 and slice thickness = 2.5 mm without gap.

Because the DSI datasets were huge, reducing the processing time, reducing the storage space, and getting better results were efficient and necessary. For each subject the following steps were applied.

First, the T2 image and the unattenuated DSI images (b_0) were coregistered using SPM, and the coregistered T2 image was normalized to the MNI space (T2-weighted template) using SPM. Thence, the translation and rotation matrix (T) was obtained from the deformation matrix of the normalization step.

Second, we applied distortion correction to the DSI datasets and reduced the original dataset to 102 points in q-space (half q-space) due to the property of symmetry in q-space. And we applied the T matrix to the corrected half DSI dataset.

After these two steps of preprocessing, the DSI datasets were approximately aligned to the MNI space, and the differences of translation and rotation among these 20 subjects were also reduced to a minimum.

Then, the LDDMM algorithm was applied to these subjects with 10 time steps, 2 iterations, smoothing (alpha) = 0.01, smoothing (gamma) = 1.0, and integration of the velocity field to generate deformation maps using the Euler method. Afterwards, a template DSI dataset was made.

We normalized the DSI datasets of all participants (targets) to this template (source) by an in-house program LDDMM package, and rearranged the b-table of the target DSI to be the same as that of the source DSI. In order to increase SNR, smooth sourcing and targeting was done. Also, a global equal mean was calculated, and the intensity of source and target was rescaled to a similar level. The LDDMM setting parameters were 10 time steps, 5 iterations to 30 iterations maximum, and smoothing parameters were set to 0.001 for both image space and q-space. Finally, we normalized the DSI datasets of 20 patients with schizophrenia and 20 normal controls to the DSI dataset of the template (Figure 10).

Later, we drew the tractography on the DSI template, and the ROIs were chosen in MARINA (Bender Institute of Neuroimaging, University of Giessen, Germany) to define cortical regions as ROIs on the Montreal Neurobiology Institute (MNI) T2 image

template (ICBM-152), the same as the manual approach. And we transformed these ROIs to DSI space by a segmentation matrix which was a parameter made by segmentation using SPM5 instead of a deformation matrix in the manual approach. There were two advantages to segmentation. First, the transformation parameter we obtained was superior because it used detailed information of WM and GM. Secondly, the parameter could do inverse transformation (Figure 11).

For bilateral ATR, the ipsilateral orbitofrontal lobe and thalamus were selected as two ROIs. For each UF, the ipsilateral orbitofrontal lobe and superior temporal and medial gyrus of the temporal lobe were selected for two ROIs. For the genu, the bilateral orbitofrontal lobe was selected as an ROI. All ROIs were selected the same way as in the manual approach. After ROIs were transformed to the template, we calculated the coordinates of the center of each ROI. And then made the ROIs ball-shaped in which the coordinates of the center were the same with the original ROI and the radius was about 3 to 5 voxels in order to integrate the tractography. The coordinates of the center of the left and right orbitofrontal cortex were (40,15,15) and (20,15,15) respectively, the coordinates of the center of the left and right thalamus were (34,38,22) and (26,38,22) respectively, and the coordinates of the center of the left and right superior temporal and medial gyrus of the temporal lobe were (46,24,10) and (13,24,10) respectively.

For the ATR, the UF, and the genu, the angle thresholds were 30°, 45°, and 35°, the same as manual approach, respectively. The step size and the track lengths were set to 1.24mm and 20~200mm, the same as manual approach. Also, the tract number of 200 for each targeted fiber tract was set to avoid incorrect tractography. After doing tractography, the tract bundles were also examined with other established anatomical landmarks shown in the atlases of tractography as a reference (Mori et al., 2005).

Then, we sampled the tractography, which was drawn on the template with the normalized individual brain using the mean path algorithm, the same as the manual approach. Finally, a profile of GFA values along the tract bundle and mean GFA values were obtained.

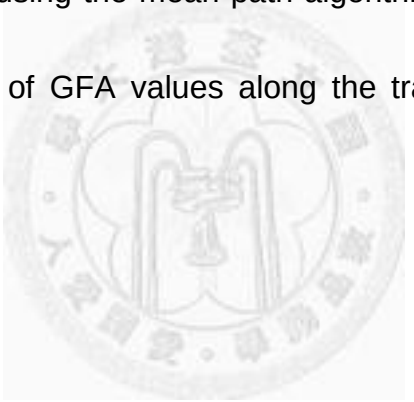

2.5. Group comparison: for two approaches

Data was analyzed using the Statistical Package for Social Sciences software version 14.0 (SPSS Inc, Chicago, IL). Age and education year distributions between the two groups were compared using the *t*-test. Statistical significance was defined as $p < 0.05$.

2.5.1. GFA

To investigate group differences in mean GFA values within the bilateral ATR, bilateral UF, and genu, analysis of independent sample t-tests were performed to evaluate the differences between groups. The significance level of between-group differences was defined as $p < 0.05$.

2.5.2. Asymmetry

Asymmetric differences in GFA values were determined for each pair of ATR and UF using a lateralization index (LI), which was calculated by the formula:

LI = (mean GFA of left side fibers – mean GFA of right side fibers) / average GFA of bilateral fibers.

The LI, indicative of left-right asymmetry, was compared between both schizophrenia and normal controls using an Independent-samples t test.

2.5.3. Association of PANSS factors

Exploratory analyses of the relationship between GFA values and clinical measures (PANSS scores), total scores for PANSS, and the five PANSS factor

subscores were computed using bivariate two-tailed Spearman's correlation coefficient. Because these analyses were exploratory in nature, we used $p < 0.05$ for statistical significance, rather than correcting for multiple correlations.

2.5.4. Comparison between two approaches

Furthermore, we investigated the correlation of the GFA value obtained from these two different approaches by Pearson correlations, and studied if the difference between these two groups could be the same in both approaches.

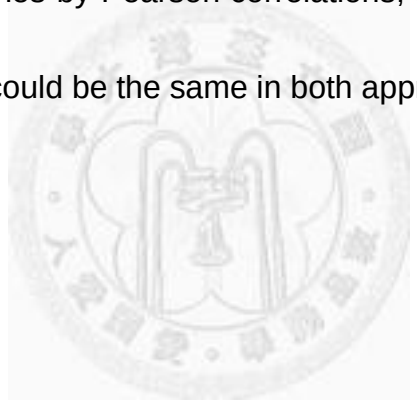

Chapter 3

Results: Manual approach

3.1. Subjects

Age and education year distributions between the two groups were compared using the *t*-test. And there were no significant differences in age distribution (p = .870) between the patients with schizophrenia and normal controls. But the education year of patients with schizophrenia was lower than the normal controls' education year (p = .000).

3.2. Mean comparison and lateralization index between patients with schizophrenia and normal controls

In the results of the manual approach, we obtained the mean GFA values of these fibers in both groups by using a manual approach, and compared the mean GFA values of these fibers between the two groups by two tailed independent sample T tests respectively. Also, the lateralization index of the ATR and UF of both groups was calculated, and was compared between the two groups by two tailed independent sample T tests respectively. And, the LI (lateralization index) of the ATR and the UF was also compared between groups by two tailed independent sample T tests respectively. These results are mentioned as following:

In ATR, the GFA value was only significantly reduced in the left side in schizophrenia patients compared to normal controls, but in the right side, we could also see the decreasing trend even through the difference was not significant (ATR_L: GFA (sch) = 0.1612 (.017), GFA (nor) = 0.2004 (.074), p = 0.048*; ATR_R: GFA (sch) = 0.1616 (.026), GFA (nor) = 0.1977 (.072), p = 0.081). However, there was no asymmetry found in either group (Schizo: p = 0.930; Normal: p = 0.908). And also, there was no significant difference between the two groups in the lateralization index (LI (sch) = 0.0182 (0.092), LI (nor) = 0.0051 (0.076), p = 0.628).

In the UF, there was a significant reduction of the mean GFA in the bilateral UF in

patients with schizophrenia as compared to the normal controls (UF_L: GFA (sch) = 0.1782 (.031), GFA (nor) = 0.2127 (.051), p = 0.033*; UF_R: GFA (sch) = 0.1616 (.029), GFA (nor) = 0.2054 (.051), p = 0.031*), and the asymmetry in both groups was not significant (Schizo: p = 0.653; Normal: p = 0.429). Also, there was no significant difference between the two groups in the lateralization index (LI (sch) = 0.020 (0.079), LI (nor) = 0.001 (0.050), p = 0.365).

In the genu, there is a significant reduction of the GFA of the genu in schizophrenia patients as compared to the controls (GFA (sch) = 0.2322 (0.031), GFA (nor) = 0.2672 (0.054), p = 0.035*) (Table 3; Figure 12).

3.3. Correlation between the PANSS factors and mean GFA values

By using the two-tailed Bivariate Spearman's correlation coefficient, we found that there was a positive correlation between GFA values of the right UF and Negative total scores (r = .481*, *p* = .037).

Moreover, we found a negative correlation between GFA values of the genu of a factor of 5 (anxiety/depression; r = - .565*, p = .015) as well as a negative correlation with total scores of general (r = -.474*, *p* = .040) (Table 4; Figure 13).

Chapter 4

Results: Automatic template-based approach

4.1. Mean comparison and lateralization index between patients with schizophrenia and normal controls

In our results of the template-based automatic approach, we sampled the tractography which was drawn on the template against the normalized individual brain using the mean path algorithm, as in the manual approach, calculated the GFA profile along the tract bundle and mean GFA values, and compared the mean GFA values of these fibers between the two groups by two tailed independent samples and the T test

respectively. Also, the lateralization index of the ATR and UF of both groups was calculated, and was compared between the two groups by a two tailed independent samples T test, respectively. And, the LI (lateralization index) of ATR and UF was also compared between groups by a two tailed independent samples T test respectively. These results were mentioned as following:

In the ATR, the GFA value was reduced in both sides in patients compared to normal controls. But the difference was not significant. (ATR_L: GFA (sch) = 0.0922 (.018), GFA (nor) = 0.0979 (.021), p = 0.367; ATR_R: GFA (sch) = 0.0910 (.019), GFA (nor) = 0.0917 (.014), p = 0.903). Also, there was no asymmetry found in both groups (Schizo: p = 0.840; Normal: p = 0.288). And also, there was no significant difference between the two groups in the lateralization index (LI (sch) = 0.0143(0.109), LI (nor) = 0.0540(0.272), p = 0.549).

In the UF, there was a reduction of the mean GFA in the bilateral UF in patients with schizophrenia as compared to the normal controls, but the reduction was not significant (UF_L: GFA (sch) = 0.1104 (.027), GFA (nor) = 0.1228 (.023), p = 0.122; UF_R: GFA (sch) = 0.1088 (.020), GFA (nor) = 0.1134 (.021), p = 0.478), and the asymmetry in both groups was not significant (Schizo: p = 0.833; Normal: p = 0.191). However, there was a significant difference between the two groups in the lateralization index (LI (sch) = -0.0006 (0.123), LI (nor) = 0.0806 (0.109), p = 0.033*).

In the genu, there is a reduction trend of GFA values of the genu in schizophrenia patients as compared to the controls, but the reduction was not significant (GFA (sch) = 0.1254 (0.028), GFA (nor) = 0.1302 (0.035), p = 0.632).

There was a trend in which all GFA values of tracts in schizophrenia were lower than the normal controls' (Table 5; Figure 14).

4.2. Analysis of GFA profile

In the automatic template approach, the tract lengths were all the same in every individual case because we used the tracts drawn on the template and sampled them to the normalized individual brain. Therefore, it was necessary to compare the GFA profile of certain tracts in a group comparison.

We calculated the average of the GFA values of certain tracts step by step for two groups respectively, and drew the GFA profile. We found something something from the profiles.

In the bilateral ATR, we could find that the GFA values were lower in the cortex (anterior) part than the thalamus (posterior) part in both groups. In left ATR, the GFA values of all steps in schizophrenia were lower than normal controls'. However, in the right ATR, the GFA values in schizophrenia were similar to the normal controls' except

of the thalamus part. Therefore, in patients with schizophrenia, the reduction of mean GFA value in right ATR was not as conspicuous as in the left ATR. This result was consistent with the manual approach where the mean GFA value was reduced significantly in left ATR but not in the right ATR in patients with schizophrenia (Figure 15).

In the bilateral UF, we could find that the highest GFA value existed on the margin of the lateral sulcus where the UF was bending from the lateral OFC to the temporal lobe. And in left UF, the GFA values in schizophrenia were almost all lower than normal controls'. But in right UF, the GFA values in schizophrenia were higher than normal controls' in lateral OFC even though lower in temporal lobe as in the left UF (Figure 16).

In the genu, we could find that the higher GFA values appeared on the intersection with the superior longitudinal fasciculus (SLF) and the cingulum bundle, and the lower GFA values appeared on the intersection with coroa radiata. The compression of fiber tracts might make the GFA value rise, and the splicing of fiber tracts might make the GFA value drop. The GFA values in schizophrenia were almost all lower than normal controls' everywhere, except the left SLF part (Figure 17).

In order to elaborate on the differences, Linear Discriminant Function Analysis was used and the discriminant coefficients were obtained. The discriminant function

coefficients are partial coefficients which could reflect the unique contribution of each variable (GFA values step by step) to the classification of the criterion variable (GFA values). The profile function curve, which maximized separation between the two groups of GFA profiles, told us if the variable was most or least discriminating between groups (Goodlett, Fletcher, Gilmore, & Gerig, 2009).

4.3. The correlation of the mean GFA values between these two approaches

The Pearson correlation coefficient of the mean GFA values between these two approaches was calculated, and the results were found to have the following characteristics:

There were positive correlations of the mean GFA values between two approaches in all tracts. And if we put all data together to see the correlation, there would be a significant positive correlation between these two approaches (r = .708**, *p* = .000) (Figure 18).

Chapter 5

Discussion

5.1. Lower GFA values of ATR, UF and genu in patients with schizophrenia

In our results, we found that the mean GFA value deceased in left ATR, bilateral UF, and genu in patients with schizophrenia as compared to normal controls'.

In ATR, Mamah *et al*. (2010) found the decreased FA in both sides of the ATR in patients with schizophrenia by DTI with the ROI approach. However, there was only significant GFA reduction in the left ATR in our results in patients with schizophrenia.

In the UF, our results are consistent with that of Price *et al*. (2008), while they

investigated the first-episode patients. However, we didn't find that the asymmetry disappeared in schizophrenia as some previous studies had (Kubicki, et al., 2002).

Our findings in the genu were consistent with the previous studies using DTI (Kubicki, et al., 2008; Shergill, et al., 2007). Kubicki used the ROI approach by mapping an already existing tractography based atlas onto their DTI data, while Shergill used the voxel-based analysis. And decreased GFA in the genu implies that the reduced connection between left and right prefrontal cortex might cause dysfunction of the brain.

Our findings show the usefulness of applying DSI and tractography to investigate white matter fiber tracts *in vivo* in schizophrenia, and thus extend our understanding of the pathophysiology of this disease.

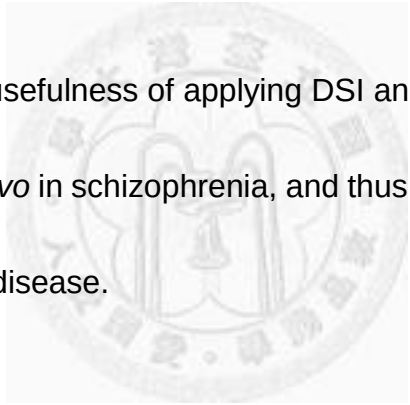

5.2. The correlation between severity of symptoms and GFA values

In our results, there was a positive correlation between GFA values of the genu and Negative total scores. The positive correlation between GFA values of right UF and Negative total scores suggestd that increased GFA in the right UF might be related to greater severity of negative symptoms. Some previous reseach revealed contrastive results that mean FA values of UF was negatively correlated with clinnical

symptoms.

In a 2005 research project, decreased fractional anisotropy in the right uncinate fasciculus are associated with personality traits and clinical symptoms of ideas of reference, suspiciousness, restricted affect, reduced extraversion and social anxiety, while those on the left side are associated with general intelligence, verbal and visual memory, and executive performance. (Nakamura, et al., 2005) This result claimed that there were different traits between the left and right UF. The function of the uncinate fasciculus was not known clearly, though it was traditionally considered to be part of the limbic system.

On the other hand, we found a negative correlation between GFA values of genu of a factor of 5 (anxiety/depression) as well as a negative correlation with General total scores. The negative correlation between GFA values of the genu of a factor of 5 (anxiety/depression) implies that reduced GFA in the genu might associate with greater severity of the anxiety and depression state. Moreover, the negative correlation between GFA values of the genu and General total scores suggestd that decreased GFA in the genu might be related to greater severity of general symptoms. This finding was consistent with our hypothesis that the integrity of the genu in schizophrenia was not as intact as that of the normal controls', and the reduced integrity of the genu resulted in the disconnection of the bilateral OFC. It inhibited

emotion-moderating function of the OFC.

However, we didn't find any correlation between mean GFA scores of the ATR and PANSS scores. In a previous study, Sussman et al (2009) also didn't find any correlation between fiber tract integrity of the ATR and psychopathology using the PANSS.

In our PANSS data, scores of some symptoms were lower, so we used factor scores which were summarized to avoid the incidental results. Also, the timing of PANSS evaluating and the issuing medication be also needed to be controlled.

5.3. The different results from the two approaches

In the manual approach, the mean GFA values of all tracts except that of the right ATR were significantly lower in patients with schizophrenia compared to normal controls'. However, in the template approach, the significant difference was absent even through there was a trend that the meant GFA values were lower in schizophrenia. Because we used intepolation calculation while normalizing to the template DSI and this step would make the ODF of the voxel smooth out.

Also, during the process of normalization, the coordinates of each voxel was changed, and the ODF of each voxel was decomposed and restructured. This

phenomenon created less anisotropy at each voxel and reduced the GFA values. The sensitivity was lower in template approach due to the process of smoothing, that means, the individual difference was not easily observed. However, the SNR was higher because the template was made from twenty subjects. With the increasing number of different subjects, the template would be more normal and general.

5.4. Template approach: group comparison of GFA profile

One advantage of template approach is that it's easier and necessary to do profile analysis due to the fact that the tract lengths were all the same. And there were some advantages of profile analysis.

First, we can undertsand the trend of GFA values along a certain tract. This allows us to know where the peak (higher GFA values) and valley (lower GFA values) are, and further investigate the anatomical location. In our genu results, the higher GFA values appeared on the intersection with the superior longitudinal fasciculus (SLF) and the cingulum bundle, and the lower GFA values was appeared on the intersection with the corona radiata. The way the genu and SLF intersected caused the genu and the cingulum bundle to be compressed and it lead to the GFA values being higher. However, the genu and the corona radiate intersected in a spliced way,

causing the GFA values to be lower.

Secondly, we could do partial comparisons step by step, and knew where the discrimination was. In our results in the right ATR, the GFA values in schizophrenia were almost all lower than normal controls' except in the thalamus section. This may give us an explanation as to why the mean GFA value of patients was lower in the left ATR but not in the right ATR in the manual approach. Also, we can find that there is a left-right asymmetry in the thalamus part of the normal controls. However, this asymmetry was absent in schizophrenic patients. The asymmetry of the profile in the thalamus may be important. It seemed that there was an asymmetry between the left and right thalamus. In 1996, the volume of the left anterior thalamus was found to be decreased by 15% in patients with schizophrenia in a post mortem study. Also, a lower metabolic rate was shown in the right thalamus in patients with schizophrenia, with a loss of the normal pattern of right larger than left asymmetry (Buchsbaum, et al., 1996). In another post mortem report, the volume as well as neuron number of the right medial pulvinar was found to be reduced by 19% in patients with schizophrenia compared to normal controls (Byne, et al., 2007). Although the asymmetry of the thalamus volume was still unclear, the reduced volumes of the thalamus relating to the increased volumes of lateral ventricles were indicated by an MRI finding (Cannon, et al., 1998), and increased volumes of lateral ventricles were commonly observed in

schizophrenia (Kempton, Stahl, Williams, & DeLisi, 2010).

Also, in our results in the genu, the GFA values in schizophrenia were almost all lower than the normal controls' everywhere except of the left SLF part. These results were interesting in that we could only get this information from the template approach.

5.5. Limitations

There were some limitations in this study. First, our sample size limited the statistical power. If the number of subjects was increased, there could be a significantly reduced mean GFA value of ATR in schizophrenia. Second, the correlation between severity of symptoms and mean GFA values were multiple comparisons, although the finding of the relationship of the genu and anxiety/depression was based on our hypothesis. In the future, increasing the number of subjects is necessary. Also, the bias resulted from two approach is not the same, we have to consider about it more.

Chapter 6

Conclusions

Our findings showed the usefulness of applying DSI and tractography to investigate white matter fiber tracts in vivo in schizophrenia; thus extending our understanding of the pathophysiology of this disease. Further studies are required to recruit more sublects and examine the gender effect on the GFA asymmetry and on the correlation with the severity of clinical symptoms. These two approaches were complementary to each other because they possessed different advantages and could support each other. Also, the individual differences of schizophrenia are variable;

comparing the variation of individuals' profiles is getting more important. In conclusion, we successfully established a flow procession of the automatic template-based approach from the template making to normalization. In the future, we will combine these two approaches in order to find the neuroinage biomarker of schizophrenia or other diseases.

References

Alexander, D. C., Pierpaoli, C., Basser, P. J., & Gee, J. C. (2001). Spatial transformations of diffusion tensor magnetic resonance images. *IEEE Trans Med Imaging, 20*(11), 1131-1139.

Ashburner, J. (2007). A fast diffeomorphic image registration algorithm. *Neuroimage, 38*(1), 95-113.

Barbas, H. (2000). Connections underlying the synthesis of cognition, memory, and emotion in primate prefrontal cortices. *Brain Res Bull, 52*(5), 319-330.

Basser, P. J., Mattiello, J., & LeBihan, D. (1994). MR diffusion tensor spectroscopy and imaging. *Biophys J, 66*(1), 259-267.

Bechara, A., Tranel, D., Damasio, H., & Damasio, A. R. (1996). Failure to respond autonomically to anticipated future outcomes following damage to prefrontal cortex. *Cereb Cortex, 6*(2), 215-225.

Beg, M. F., Miller, M. I., Trouve, A., & Younes, L. (2005). Computing large deformation metric mappings via geodesic flows of diffeomorphisms. *International Journal of Computer Vision, 61*(2), 139-157.

Buchsbaum, M. S., Someya, T., Teng, C. Y., Abel, L., Chin, S., Najafi, A., et al. (1996). PET and MRI of the thalamus in never-medicated patients with schizophrenia. *Am J Psychiatry, 153*(2), 191-199.

Butter, C. M., & Snyder, D. R. (1972). Alterations in aversive and aggressive behaviors following orbital frontal lesions in rhesus monkeys. *Acta Neurobiol Exp (Wars), 32*(2), 525-565.

Byne, W., Fernandes, J., Haroutunian, V., Huacon, D., Kidkardnee, S., Kim, J., et al. (2007). Reduction of right medial pulvinar volume and neuron number in schizophrenia. *Schizophr Res, 90*(1-3), 71-75.

Byne, W., Hazlett, E. A., Buchsbaum, M. S., & Kemether, E. (2009). The thalamus and schizophrenia: current status of research. *Acta Neuropathol, 117*(4), 347-368.

Callaghan, P. T., Coy, A., Macgowan, D., Packer, K. J., & Zelaya, F. O. (1991). Diffraction-Like Effects in Nmr Diffusion Studies of Fluids in Porous Solids. *Nature, 351*(6326), 467-469.

Cannon, T. D., van Erp, T. G., Huttunen, M., Lonnqvist, J., Salonen, O., Valanne, L., et al. (1998). Regional gray matter, white matter, and cerebrospinal fluid distributions in schizophrenic patients, their siblings, and controls. *Arch Gen Psychiatry, 55*(12), 1084-1091.

Chiang, W.Y., Wang, H.L., Huang, S.C., Yeh, F.C., Tseng, W.Y.I., 2007.Tract-specific analysis of human white matter: mean-path based method. In proceedings of the16th Triennial Conference for the International Society of Magnetic Resonance., October 14-19, Kenting, Taiwan.

Davenport, N. D., Karatekin, C., White, T., & Lim, K. O. (2010). Differential fractional anisotropy abnormalities in adolescents with ADHD or schizophrenia. *Psychiatry Res, 181*(3), 193-198.

E. L. Hahn, “Spin echoes,” *Physical Review,* Vol. 80, pp. 580-594, 1950.

Francis, S., Rolls, E. T., Bowtell, R., McGlone, F., O'Doherty, J., Browning, A., et al. (1999). The representation of pleasant touch in the brain and its relationship with taste and olfactory areas. *Neuroreport, 10*(3), 453-459.

Friston, K. J. (1998). The disconnection hypothesis. *Schizophr Res, 30*(2), 115-125.

Funai, A. K., Fessler, J. A., Yeo, D. T., Olafsson, V. T., & Noll, D. C. (2008). Regularized field map estimation in MRI. *IEEE Trans Med Imaging, 27*(10), 1484-1494.

Goodlett, C. B., Fletcher, P. T., Gilmore, J. H., & Gerig, G. (2009). Group analysis of DTI fiber tract statistics with application to neurodevelopment. *Neuroimage,*

45(1 Suppl), S133-142.

Harrison, P. J., & Weinberger, D. R. (2005). Schizophrenia genes, gene expression, and neuropathology: on the matter of their convergence. *Mol Psychiatry, 10*(1), 40-68; image 45.

Hsu, Y. C., Hsu, C. H., & Tseng, W. Y. (2009). Correction for susceptibility-induced distortion in echo-planar imaging using field maps and model-based point spread function. *IEEE Trans Med Imaging, 28*(11), 1850-1857.

Hulshoff Pol, H. E., Schnack, H. G., Mandl, R. C., Cahn, W., Collins, D. L., Evans, A. C., et al. (2004). Focal white matter density changes in schizophrenia: reduced inter-hemispheric connectivity. *Neuroimage, 21*(1), 27-35.

Jones, D. K., Catani, M., Pierpaoli, C., Reeves, S. J., Shergill, S. S., O'Sullivan, M., et al. (2006). Age effects on diffusion tensor magnetic resonance imaging tractography measures of frontal cortex connections in schizophrenia. *Hum Brain Mapp, 27*(3), 230-238.

Kanaan, R. A., Shergill, S. S., Barker, G. J., Catani, M., Ng, V. W., Howard, R., et al. (2006). Tract-specific anisotropy measurements in diffusion tensor imaging. *Psychiatry Res, 146*(1), 73-82.

Kay, S. R., Fiszbein, A., & Opler, L. A. (1987). The positive and negative syndrome scale (PANSS) for schizophrenia. *Schizophr Bull, 13*(2), 261-276.

Kay, S. R., & Sevy, S. (1990). Pyramidical model of schizophrenia. *Schizophr Bull, 16*(3), 537-545.

Kempton, M. J., Stahl, D., Williams, S. C., & DeLisi, L. E. (2010). Progressive lateral ventricular enlargement in schizophrenia: a meta-analysis of longitudinal MRI studies. *Schizophr Res, 120*(1-3), 54-62.

Konick, L. C., & Friedman, L. (2001). Meta-analysis of thalamic size in schizophrenia. *Biol Psychiatry, 49*(1), 28-38.

Kringelbach, M. L. (2005). The human orbitofrontal cortex: linking reward to hedonic experience. *Nat Rev Neurosci, 6*(9), 691-702.

Kubicki, M., Styner, M., Bouix, S., Gerig, G., Markant, D., Smith, K., et al. (2008). Reduced interhemispheric connectivity in schizophrenia-tractography based segmentation of the corpus callosum. *Schizophr Res, 106*(2-3), 125-131.

Kubicki, M., Westin, C. F., Maier, S. E., Frumin, M., Nestor, P. G., Salisbury, D. F., et al. (2002). Uncinate fasciculus findings in schizophrenia: a magnetic resonance diffusion tensor imaging study. *Am J Psychiatry, 159*(5), 813-820.

Kuo, L. W., Lee, C. Y., Chen, J. H., Wedeen, V. J., Chen, C. C., Liou, H. H., et al. (2008). Mossy fiber sprouting in pilocarpine-induced status epilepticus rat hippocampus: a correlative study of diffusion spectrum imaging and histology. *Neuroimage, 41*(3), 789-800.

Kuo, L.W., Chen, J.H., Wedeen, V.J., Tseng, W.Y.I., 2008. Optimization of diffusion spectrum imaging and q-ball imaging on clinical MRI system. Neuroimage 41, 7-18.

Kuo, L.W., Chiang, W.Y., Yeh, F.C., Wedeen, V.J., Tseng, W.Y.I., 2010. Optimization of Body-Centered-Cubic Encoding Scheme for Diffusion Spectrum Imaging. The International Society for Magnetic Resonance in Medicine Stockholm, Sweden, p.1501

Le Bihan, D. (1995). Molecular diffusion, tissue microdynamics and microstructure. *NMR Biomed, 8*(7-8), 375-386.

Le Bihan, D., Breton, E., Lallemand, D., Grenier, P., Cabanis, E., & Laval-Jeantet, M. (1986). MR imaging of intravoxel incoherent motions: application to diffusion and perfusion in neurologic disorders. *Radiology, 161*(2), 401-407.

Lin, C.P., Wedeen, V.J., Chen, J.H., Yao, C., Tseng, W.Y., 2003. Validation of diffusion spectrum magnetic resonance imaging with manganese-enhanced rat

optic tracts and ex vivo phantoms. Neuroimage 19, 482-495.

Liu, I. C., Chiu, C. H., Chen, C. J., Kuo, L. W., Lo, Y. C., & Tseng, W. Y. (2010). The microstructural integrity of the corpus callosum and associated impulsivity in alcohol dependence: a tractography-based segmentation study using diffusion spectrum imaging. *Psychiatry Res, 184*(2), 128-134.

Lopez-Bendito, G., & Molnar, Z. (2003). Thalamocortical development: how are we going to get there? *Nat Rev Neurosci, 4*(4), 276-289.

Mori, S., Wakana, S., Lidia, M., van Zijl, P., 2005. MRI Atlas of Human White Matter. Elsevier, Amsterdam.

Moseley, M. E., Cohen, Y., Mintorovitch, J., Chileuitt, L., Shimizu, H., Kucharczyk, J., et al. (1990). Early detection of regional cerebral ischemia in cats: comparison of diffusion- and T2-weighted MRI and spectroscopy. *Magn Reson Med, 14*(2), 330-346.

Nakamura, M., McCarley, R. W., Kubicki, M., Dickey, C. C., Niznikiewicz, M. A., Voglmaier, M. M., et al. (2005). Fronto-temporal disconnectivity in schizotypal personality disorder: a diffusion tensor imaging study. *Biol Psychiatry, 58*(6), 468-478.

Norman, R. M., Malla, A. K., Williamson, P. C., Morrison-Stewart, S. L., Helmes, E., & Cortese, L. (1997). EEG coherence and syndromes in schizophrenia. *Br J Psychiatry, 170*, 411-415.

Price, G., Cercignani, M., Parker, G. J., Altmann, D. R., Barnes, T. R., Barker, G. J., et al. (2008). White matter tracts in first-episode psychosis: a DTI tractography study of the uncinate fasciculus. *Neuroimage, 39*(3), 949-955.

Rolls, E. T. (2004). The functions of the orbitofrontal cortex. *Brain Cogn, 55*(1), 11-29.

Rosenberger, G., Kubicki, M., Nestor, P. G., Connor, E., Bushell, G. B., Markant, D., et al. (2008). Age-related deficits in fronto-temporal connections in schizophrenia:

a diffusion tensor imaging study. *Schizophr Res, 102*(1-3), 181-188.

Rowland, L. M., Spieker, E. A., Francis, A., Barker, P. B., Carpenter, W. T., & Buchanan, R. W. (2009). White matter alterations in deficit schizophrenia. *Neuropsychopharmacology, 34*(6), 1514-1522.

Scholz, J., Klein, M. C., Behrens, T. E., & Johansen-Berg, H. (2009). Training induces changes in white-matter architecture. *Nat Neurosci, 12*(11), 1370-1371.

Segal, D., Koschnick, J. R., Slegers, L. H., & Hof, P. R. (2007). Oligodendrocyte pathophysiology: a new view of schizophrenia. *Int J Neuropsychopharmacol, 10*(4), 503-511.

Seok, J. H., Park, H. J., Chun, J. W., Lee, S. K., Cho, H. S., Kwon, J. S., et al. (2007). White matter abnormalities associated with auditory hallucinations in schizophrenia: a combined study of voxel-based analyses of diffusion tensor imaging and structural magnetic resonance imaging. *Psychiatry Res, 156*(2), 93-104.

Shergill, S. S., Kanaan, R. A., Chitnis, X. A., O'Daly, O., Jones, D. K., Frangou, S., et al. (2007). A diffusion tensor imaging study of fasciculi in schizophrenia. *Am J Psychiatry, 164*(3), 467-473.

Stejskal EO;Tanner JE (1964). Spin Diffusion Measurements:Spin Echoes in the Presence of a Time-Dependent Field Gradient. *Journal of Chemical Physics*

Sussmann, J. E., Lymer, G. K., McKirdy, J., Moorhead, T. W., Munoz Maniega, S., Job, D., et al. (2009). White matter abnormalities in bipolar disorder and schizophrenia detected using diffusion tensor magnetic resonance imaging. *Bipolar Disord, 11*(1), 11-18.

Takayanagi, Y., Takahashi, T., Orikabe, L., Masuda, N., Mozue, Y., Nakamura, K., et al. (2010). Volume reduction and altered sulco-gyral pattern of the orbitofrontal cortex in first-episode schizophrenia. *Schizophr Res, 121*(1-3), 55-65.

Torrey, H.C. Bloch equation with diffusion terms. Journal of Chemical Physics 104[3], 563-565. 1956

Tuch, D. S. (2004). Q-ball imaging. *Magn Reson Med, 52*(6), 1358-1372.

Walterfang, M., Wood, S. J., Velakoulis, D., & Pantelis, C. (2006). Neuropathological, neurogenetic and neuroimaging evidence for white matter pathology in schizophrenia. *Neurosci Biobehav Rev, 30*(7), 918-948.

Wedeen, V. J., Hagmann, P., Tseng, W. Y., Reese, T. G., & Weisskoff, R. M. (2005). Mapping complex tissue architecture with diffusion spectrum magnetic resonance imaging. *Magn Reson Med, 54*(6), 1377-1386.

Wesbey, G. E., Moseley, M. E., & Ehman, R. L. (1984). Translational molecular self-diffusion in magnetic resonance imaging. II. Measurement of the self-diffusion coefficient. *Invest Radiol, 19*(6), 491-498.

Y-C. Hsu, C-H. Hsu, and W-Y. Tseng. Spatial Normalization of Diffusion Spectrum Imaging Using Large Deformation Diffeomorphic Metric Mapping. Proc: ISMRM-ESMRMB Joint Annual Meeting, 1-7 May, 2010.

Y-C. Hsu, C-H. Hsu, and W-Y. I. Tseng. Diffeomorphic normalization via constant acceleration field.17th Scientific Meeting & Exhibition, Honolulu, Hawai'i, USA 18-24 April 2009.

Yeh, F.C., Wedeen, V.J., Tseng, W.Y.I., 2008. A recursive algorithm to decompose orientation distribution function and resolve intra-voxel fiber directions. In proceedings of the 16th Scientific Meeting and Exhibition for the International Society for Magnetic Resonance in Medicine, May 3-9, Toronto, Canada.

鄭若瑟 何海 張景瑞 藍先元 胡海國 活性與負性症狀量表(PANSS)：中文版本建立及信度研究 zh-TW 1996 中華精神醫學, 1996;10:251-258

Figures and Tables

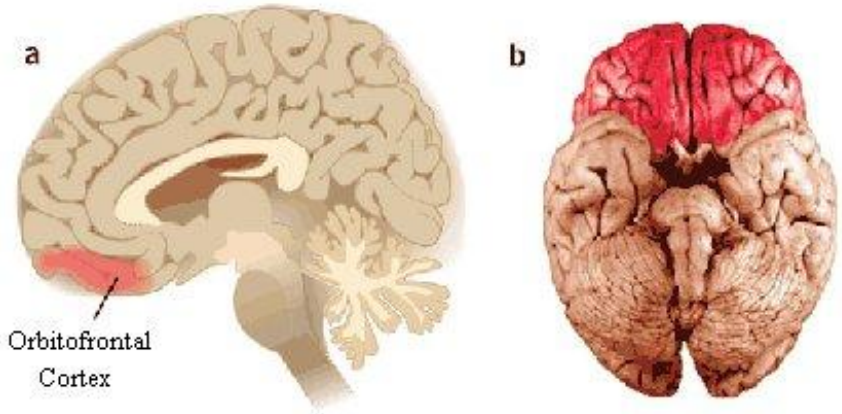

Figure 1. Orbitofrontal cortex. It consists of Brodmann area 10, 11and 47. Because of its functions in emotion and reward, the OFC is considered by some to be a part of the limbic system. A: Saggital view. B: ventral view. (Adapted from Ann Thomson, 2006)

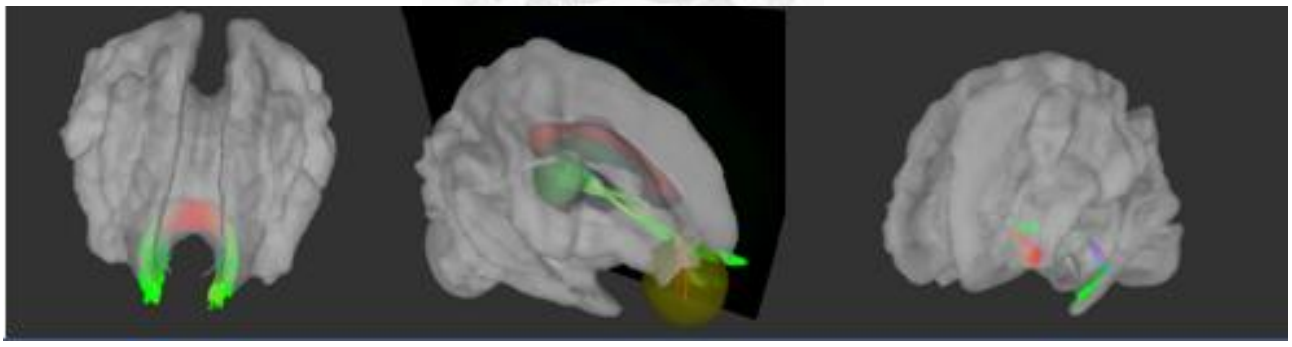

Figure 2. Three tracts selected in our research. The genu, which is the anterior part of corpus callosum connecting the left and right prefrontal cortex, is a commissural fiber (Left). The anterior thalamic radiation (ATR), which is projecting from the anterior nuclei of thalamus to the prefrontal cortex, is a projection fiber (Medium). The uncinate fasciculus (UF), which connects the prefrontal and temporal cortex of each brain hemisphere, is an association fiber (Right).

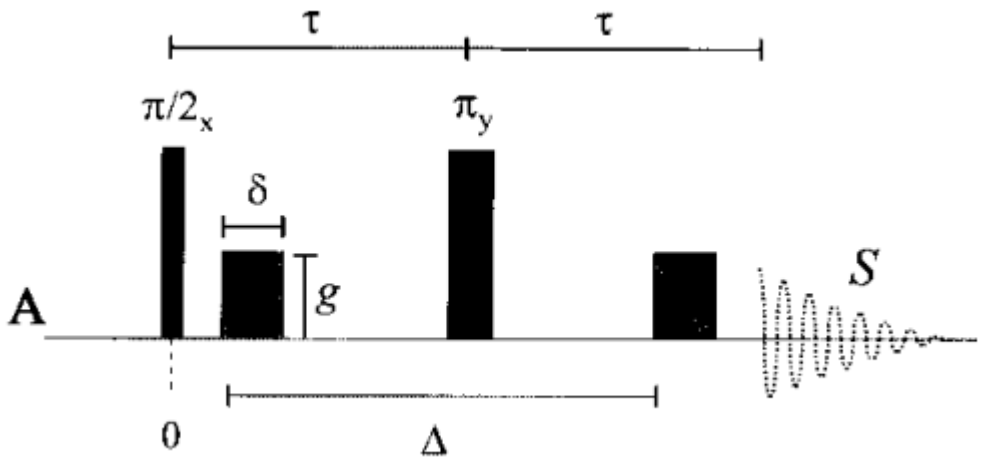

Figure 3. The pulse sequence diagram of PGSE diffusion MRI sequence. Two diffusion gradients were implemented between 90 and 180 degree RF pulse, 180 degree RF pulse and echo. If water molecules diffuse btween these two diffusion gradient, the phase can't be refocused by the second diffusion gradient. The signal will be attenuated due to the dispersion of the proton spins at the echo time.

(Adapted from Price, 2002)

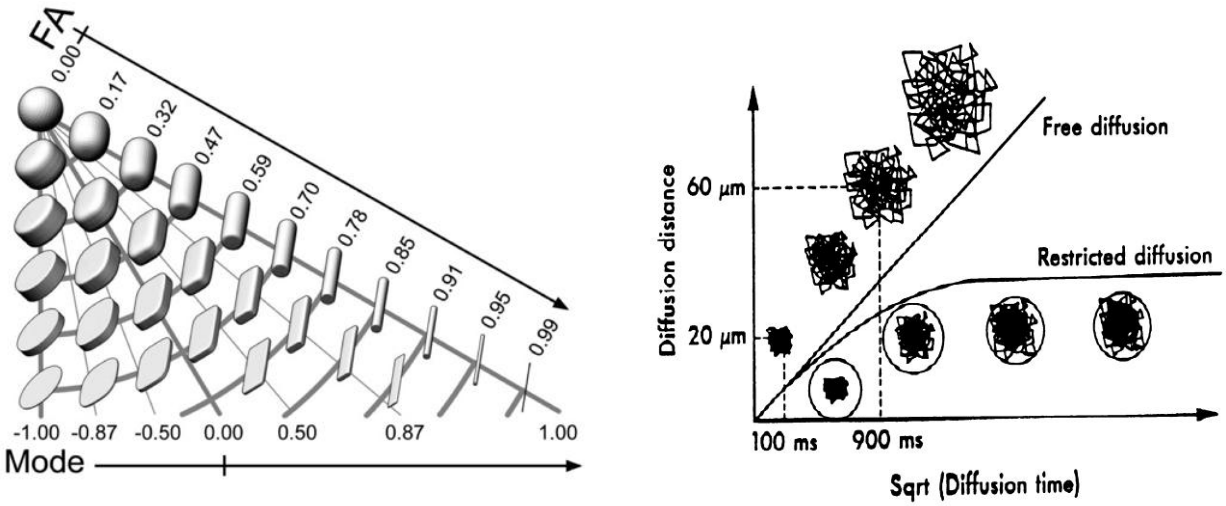

Figure 4. Fractional anisotropy. If the first eigenvalue is one and other two are zero, the value of FA will be one, and that presents the water diffusion is extremely anisotropy. If the three eigenvalues are all the same, the value of FA will be zero, and that presents the water diffusion is isotropy. Thence, a higher value of FA reflects a higher fiber density, larger axonal diameter, and higher level of consistent myenation of the brain white matter. (Adapt from Daniel B. Ennis, 2006 (Left) and Douek, 1991 (Right))

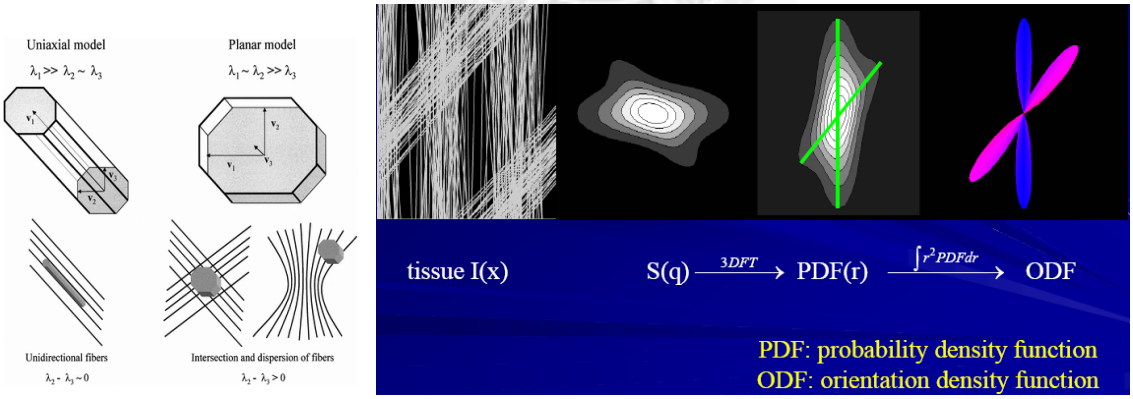

Figure 5. Crossing and kissing fibers. DSI provides the information of the probability distribution of water molecular displacement at each voxel. Then the reconstructed tractography based on DSI can solve the problem of crossing or missing fibers at each voxel. (Adapt from Douek, 1991 (Left) and W-Y. I. Tseng, 2008 (Right))

	Schizophrenia	Normal
Handiness (L:R)	1:19	0:20
Age	28 ± 7.6 years	27.9 ± 7.52 years
Education	13.4 ± 2.11 years	16.28 ± 1.78 years

Table1. The information of subjects. There is no significant difference in handiness and age between two groups. But the education year is higher of normal controls.

	DSI	T2-weighted image
Time	16min29s	2min14s
Max b-value	4000	NA
Directions	102	NA
TE	130ms	101ms
TR	9600ms	9430ms
FOV	200×200 mm^2	248x248 mm^2
Matrix size	80×80	256x256
Slice thickness	2.5mm	3mm
Slice #	56	43

Table 2. MR parameters of DSI and T2-weighted imaging. (DSI: diffusion spectrum imaging; FOV: field of view; TR: repetition time; TE: echo time; #: number)

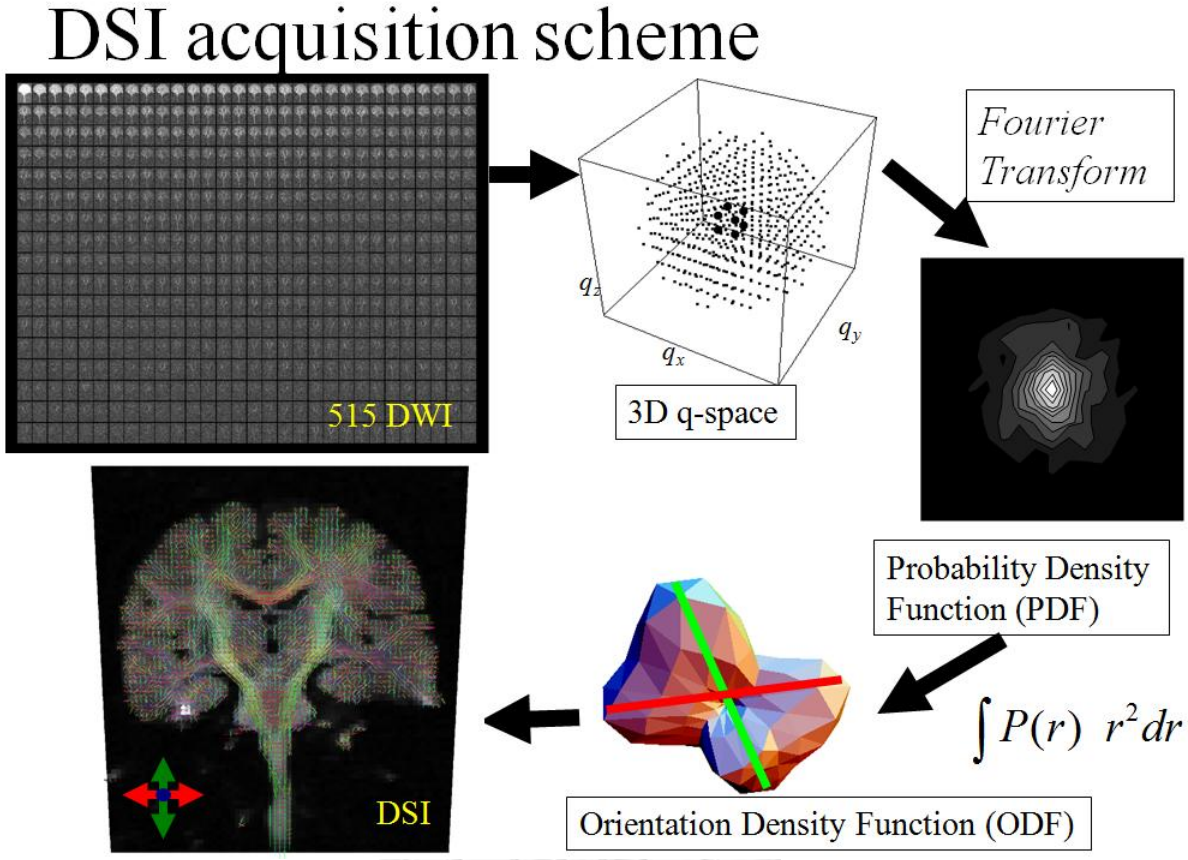

Figure 6. The flowchart of DSI. The echo signal S(q) and diffusion probability density function P(r) were a Fourier pairs, the diffusion probability density function P(r) was obtained from the echo signal S(q) which sampled to the 3D q-space by Fourier transform. To obtain PDF, the whole data in the q-space which was applied to a Hanning filter of 17 in width was performed 3D Fourier transform. And, the orientation distribution function (ODF) was calculated by taking the second moment of P(r) along each radial direction. To find out the fiber orientations at each voxel, we used an iterative way to decompose the ODF into several partial Gaussian ODFs corresponding to the primary orientations at each voxel. (Adapt from W-Y. I. Tseng, 2008)

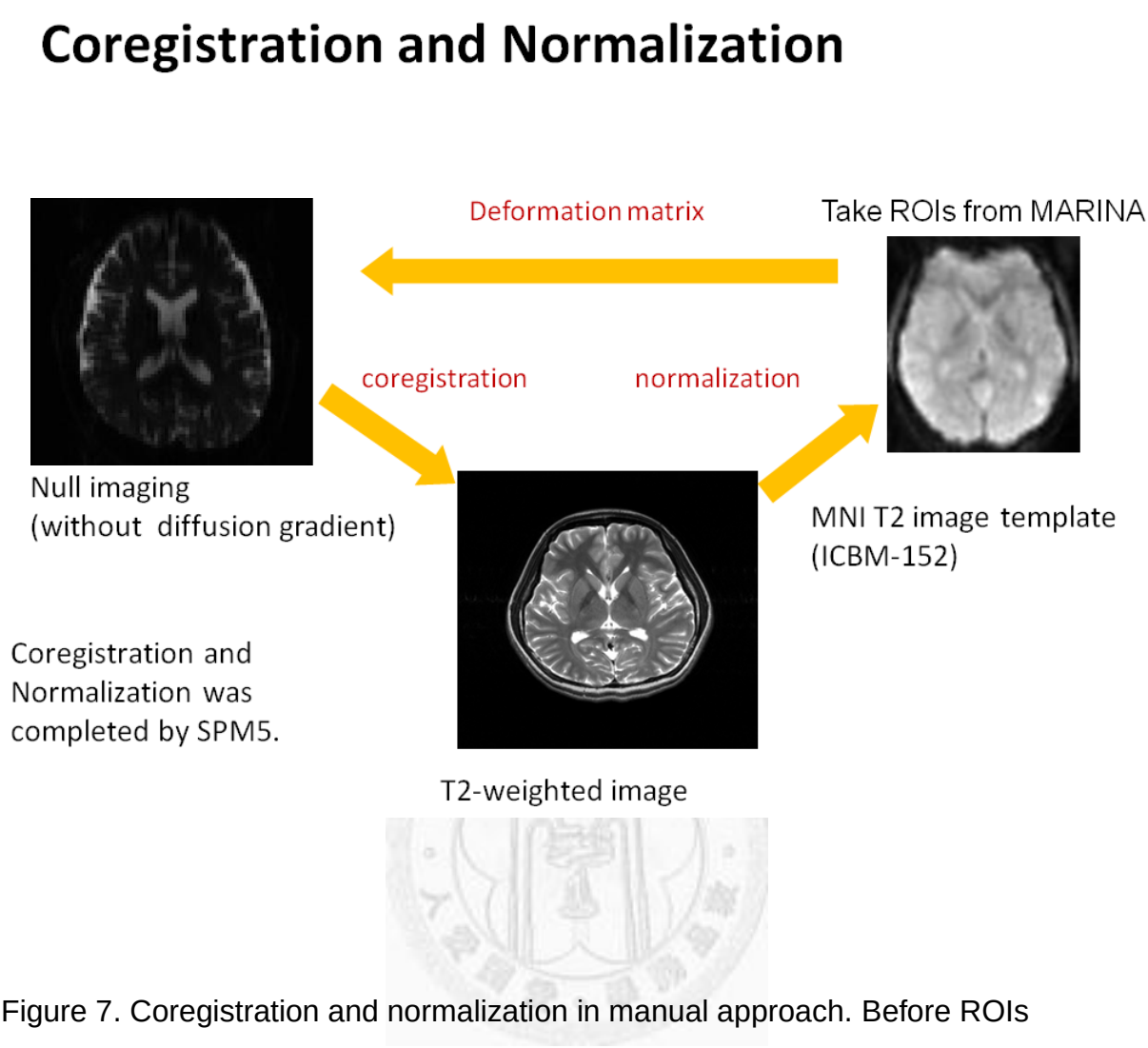

Figure 7. Coregistration and normalization in manual approach. Before ROIs selecting, we performed coregistration which is a linear transformation between the null images of DSI (b_0) of each individual participant' brain and their T2 weighted image by a 3D affine transformation matrix. And also, we performed nomalization which is a non-linear transformation from the T2 weighted image of each individual participant' brain to the Montreal Neurobiology Institute (MNI) T2 weighted image template. Thence, we got a deformation matrix in order to do inverse transformation from the coordinates of the region of interests (ROIs) defined in the MNI template to each individual participant' brain.

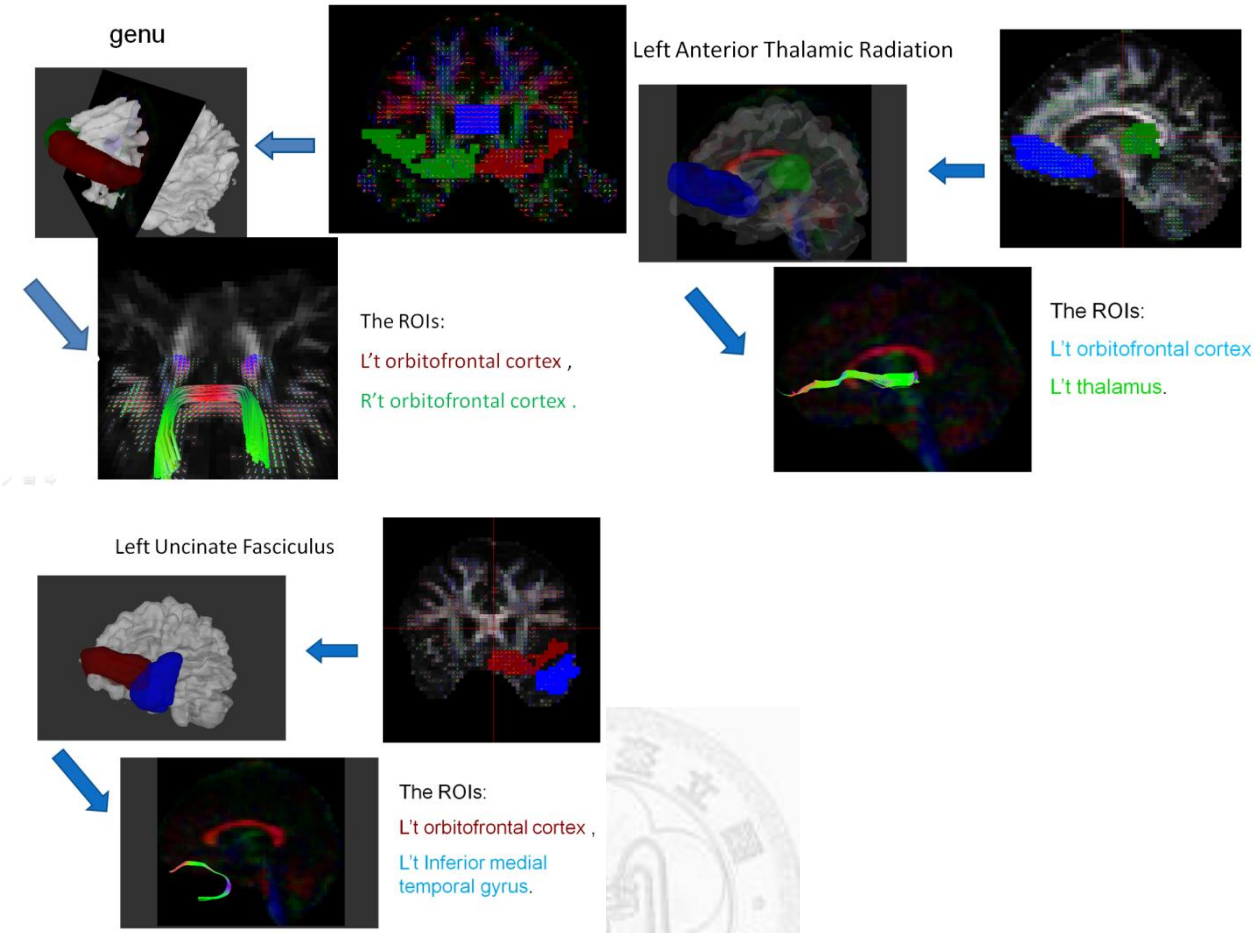

Figure 8. ROI selection and tractography. For genu, the bilateral orbitofrontal lobe was selected for two ROIs. For each UF, the ipslateral orbitofrontal lobe and Superior temporal and medial gyrus of temporal lobe were selected for two ROIs. For bilateral ATR, the ipsilateral orbitofrontal lobe and thalamus were selected for two ROIs.

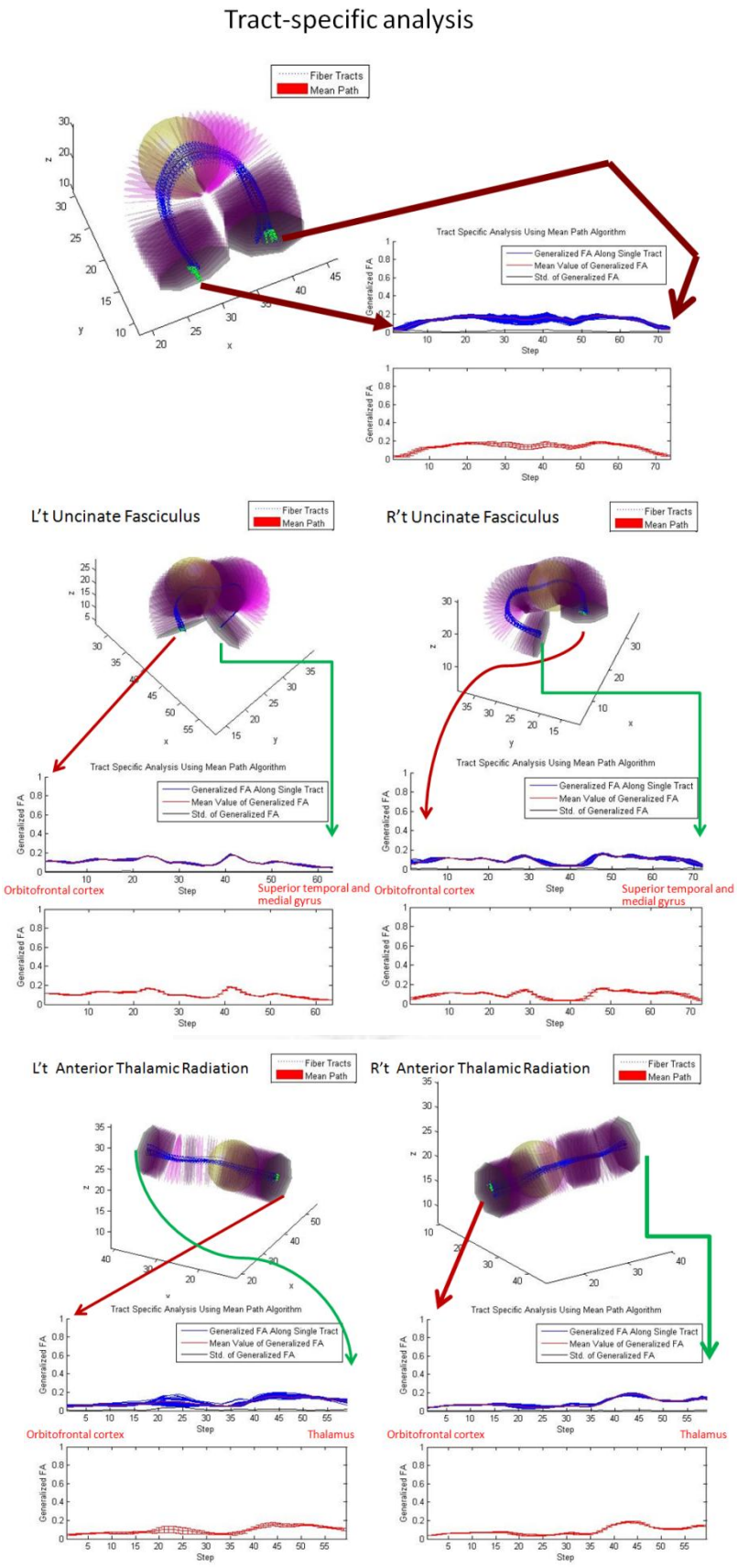

Figure 9. Mean path algorithm and GFA profile. Top: genu; Medium: uncinate fasciculus; Bottom: anterior thalaic radiation.

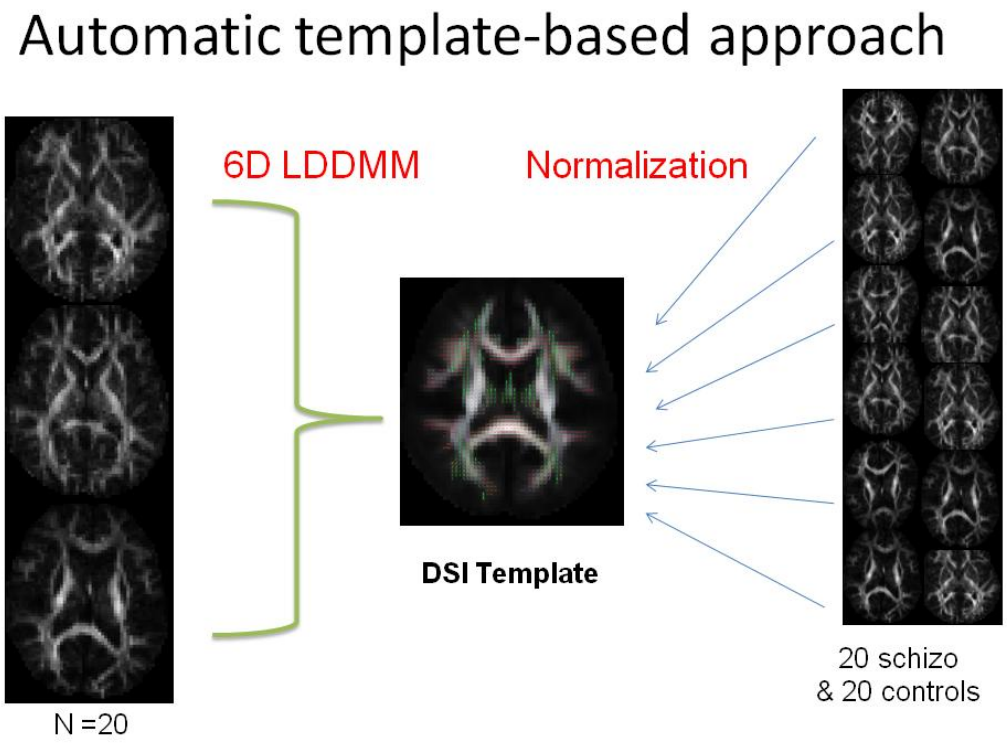

Figure 10. The template of automatic template-based approach. In the template-based automatic approach, we made a template for DSI data normalization. The template we used was made from 20 healthy subjects by using 6D LDDMM algorithm. Later, we normalized the DSI datasets of 20 patients with schizophrenia and 20 normal controls to DSI dataset of the template.

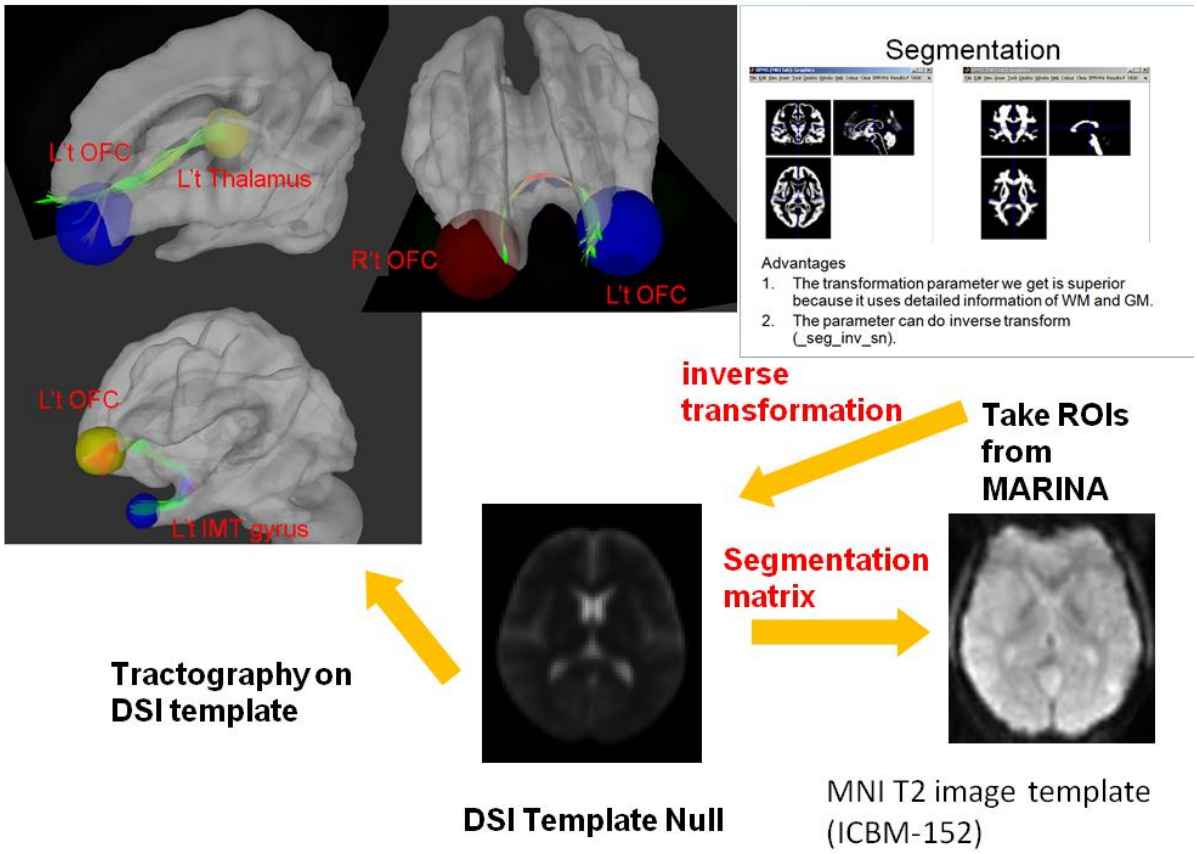

Figure 11. Tractography of the template. We did the tractography on the DSI template, and the ROIs were choosed in MARINA to define cortical regions as ROIs on the MNI T2 image template as the same as manual approach. And we transformed these ROIs to DSI space by a segmentation matrix There were two advantages of segmentation. The first, the transformation parameter we got was superior because it used detailed information of WM and GM. The second, the parameter could do inverse transformation.

	ATR_L	ATR_R	UF_L	UF_R	Genu
Schizo	0.1612(.017)	0.1616(.026)	0.1782(.031)	0.2048(.029)	0.2322(.031)
Normal	0.2004(.074)	0.1977(.072)	0.2127(.051)	0.2054(.051)	0.2672(.054)
p value	p = .048*	p = .081	p = .033*	p = .031*	p = .048*

Table 3. The results of manual approach in group comparison. The GFA values were significant reduced in all tracts unless right ATR in schizophrenia.

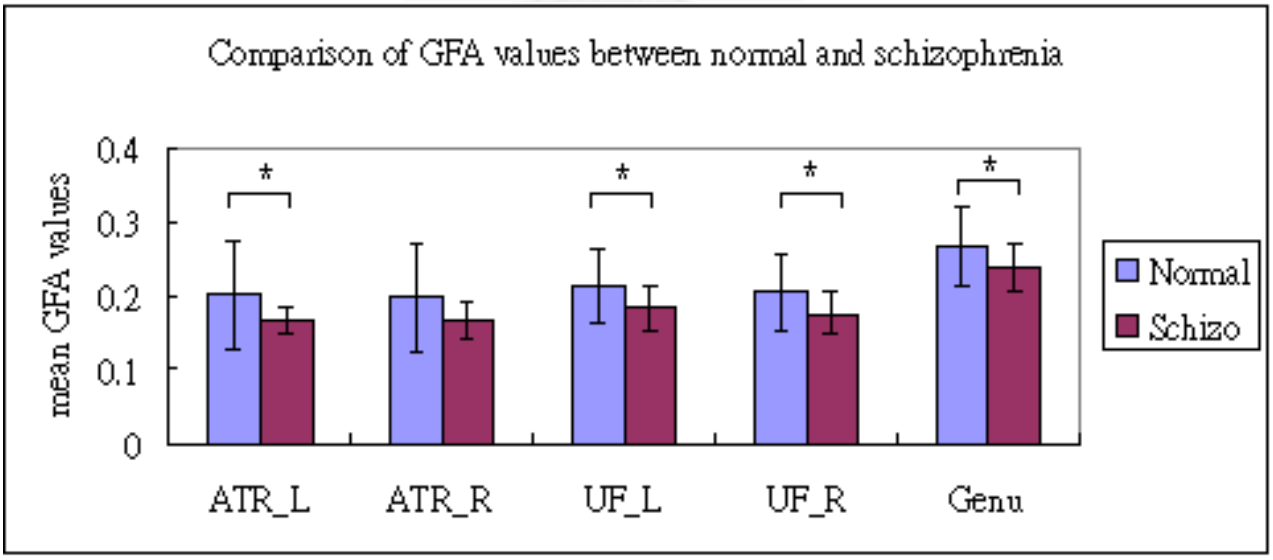

Figure 12. Comparison of mean GFA values between two groups in manual approach.

Correlations between GFA values and PANSS scores

PANSS scores	ATR_L	ATR_R	UF_L	UF_R	Genu
Total	r = -.283 *p* = .241	r = -.127 *p* = .604	r = -.083 *p* = .734	r = .245 *p* = .312	r = -.277 *p* = .250
Positive	r = -.226 *p* = .352	r = -.059 *p* = .809	r = .004 *p* = .986	r = .146 *p* = .550	r = -.266 *p* = .271
Negative	r = .107 *p* = .664	r = .141 *p* = .564	r = .243 *p* = .315	r = .481* *p* = .037	r = .236 *p* = .332
general	r = -.419 *p* = .074	r = -.292 *p* = .225	r = -.268 *p* = .267	r = -.011 *p* = .966	r = -.474* *p* = .040
Negative symptoms	r = -.061 *p* = .804	r = .076 *p* = .757	r = .085 *p* = .729	r = .358 *p* = .132	r = .054 *p* = .826
Positive symptoms	r = -.242 *p* = .319	r = -.093 *p* = .704	r = -.057 *p* = .817	r = .165 *p* = .499	r = -.298 *p* = .216
Disorganized thought	r = -.422 *p* = .072	r = -.323 *p* = .178	r = -.238 *p* = .327	r = .088 *p* = .721	r = -.354 *p* = .137
Uncontrolled hostility/excitement	r = -.085 *p* = .731	r = -.068 *p* = .783	r = .072 *p* = .768	r = .147 *p* = .549	r = -.224 *p* = .357
Anxiety/depression	r = -.167 *p* = .493	r = -.159 *p* = .515	r = -.118 *p* = .630	r = -.068 *p* = .783	r = -.462 *p* = .046

*. Correlation is significant at the 0.05 level (2-tailed).

Table 4. The correlations between mean GFA values and PANSS scores in manual approach.

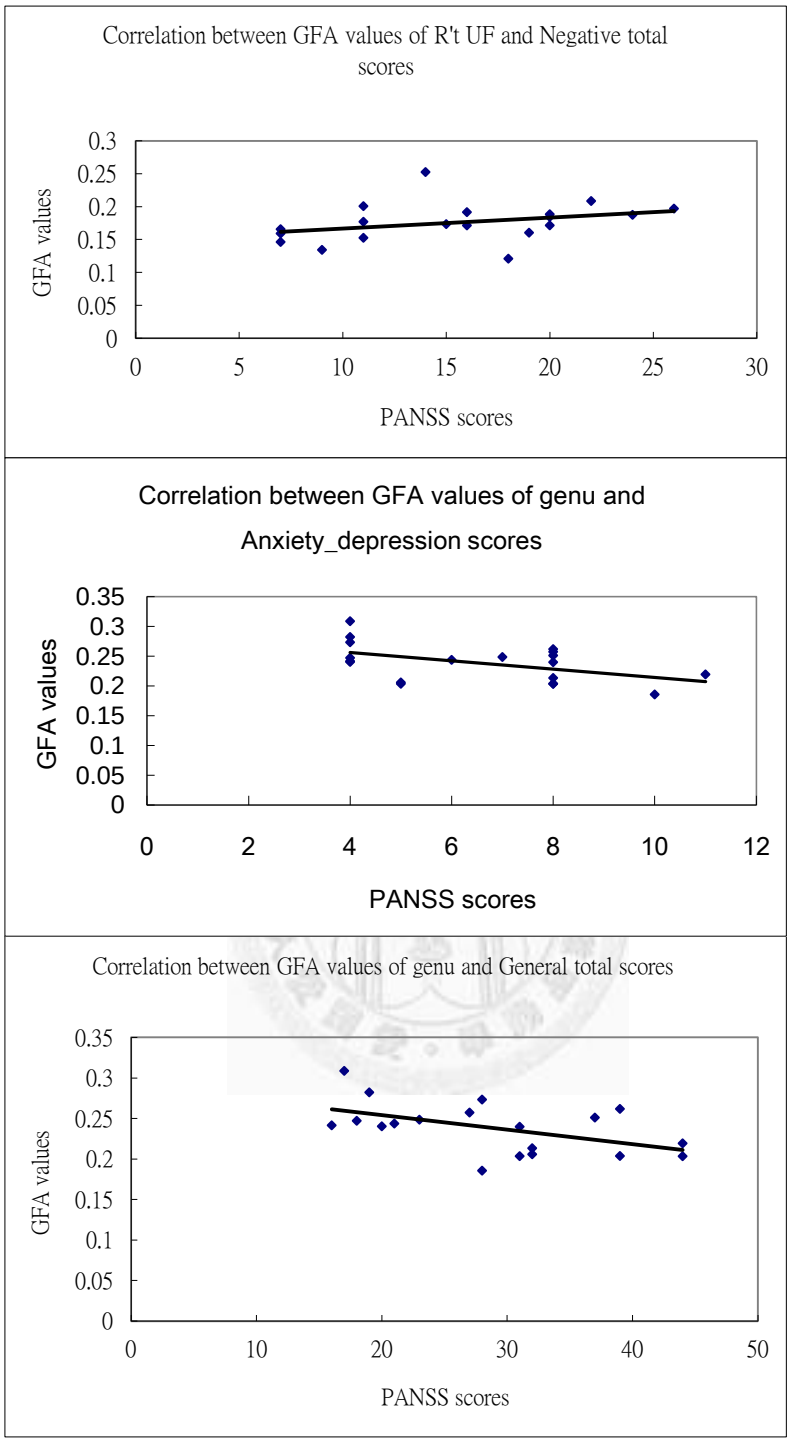

Figure 13. Correlations between PANSS and GFA. There was a positive correlation between GFA values of right UF and Negative total scores (r = .481*, *p* = .037) (Top). Moreover, we found a negative correlation between GFA values of genu and the factor 5 (anxiety/depression; r = - .565*, p = .015)(Medium) as well as a negative correlation with total scores of general (r = -.474*, *p* = .040).(Bottom)

	ATR_L	ATR_R	UF_L	UF_R	Genu
Schizo	0.0922(.017)	0.0910(.019)	0.1104(.027)	0.1088(.020)	0.1254(.028)
Normal	0.0979(.021)	0.0917(.014)	0.1228(.023)	0.1134(.021)	0.1302(.035)
p value	p = .367	p = .903	p = .122	p = .478	p = .632

Table 5. The results of automatic template-based approach in group comparison. There was a trend that all GFA values of tracts in schizophrenia were lower than normal controls'.

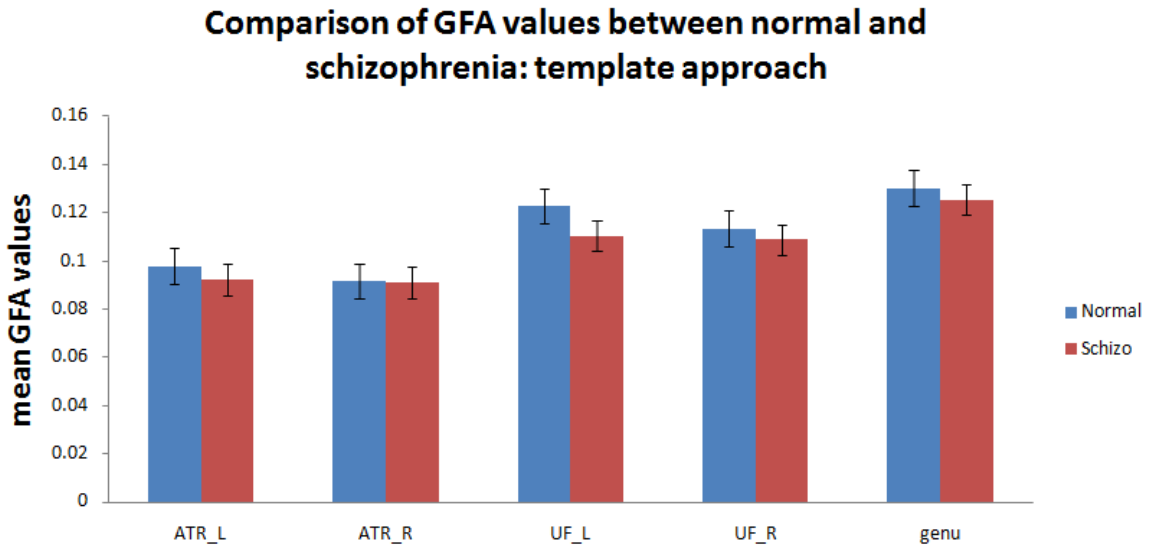

Figure 14. Comparison of mean GFA values between two groups in automatic template-based approach.

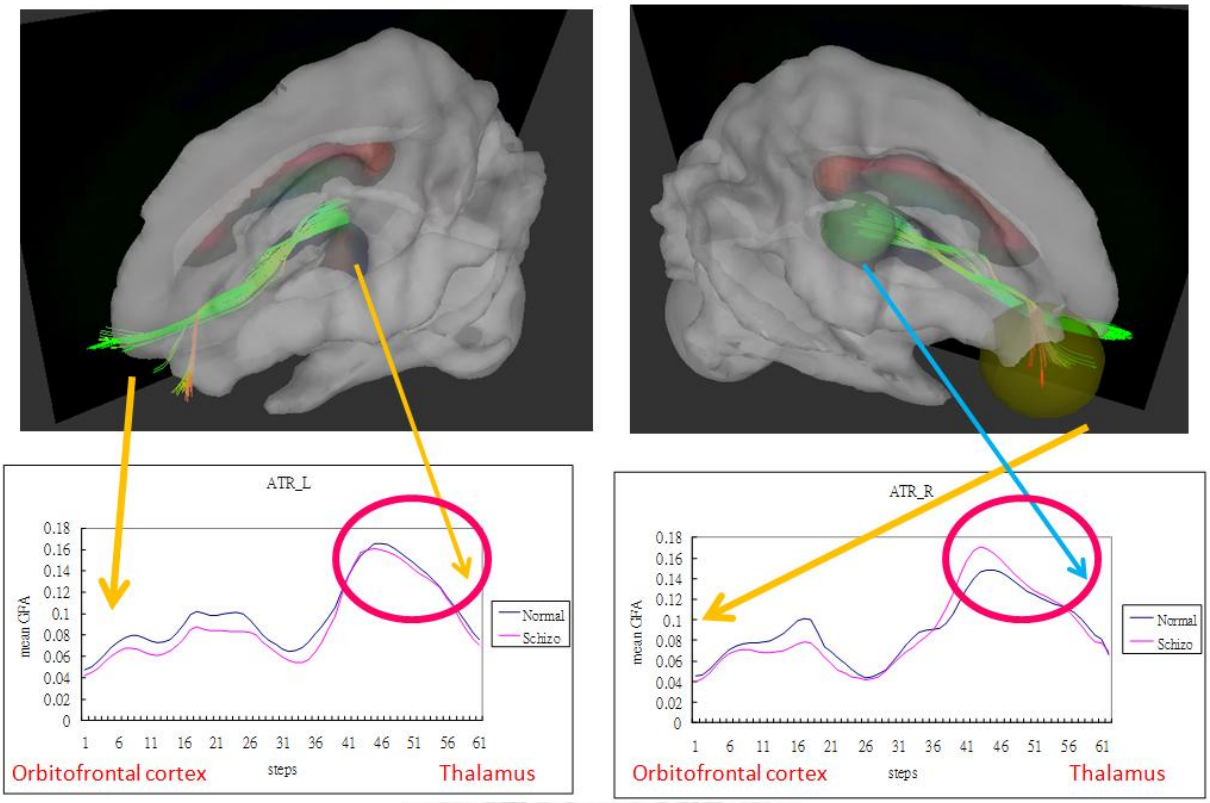

Figure 15. GFA profile of ATR. In bilateral ATR, we could find that the GFA values were lower in the cortex (anterior) part than the thalamus (posterior) part in both groups. In left ATR, the GFA values of all steps in schizophrenia were lower than normal controls'. However, in right ATR, the GFA values in schizophrenia were almost lower than normal controls' except of the thalamus part.

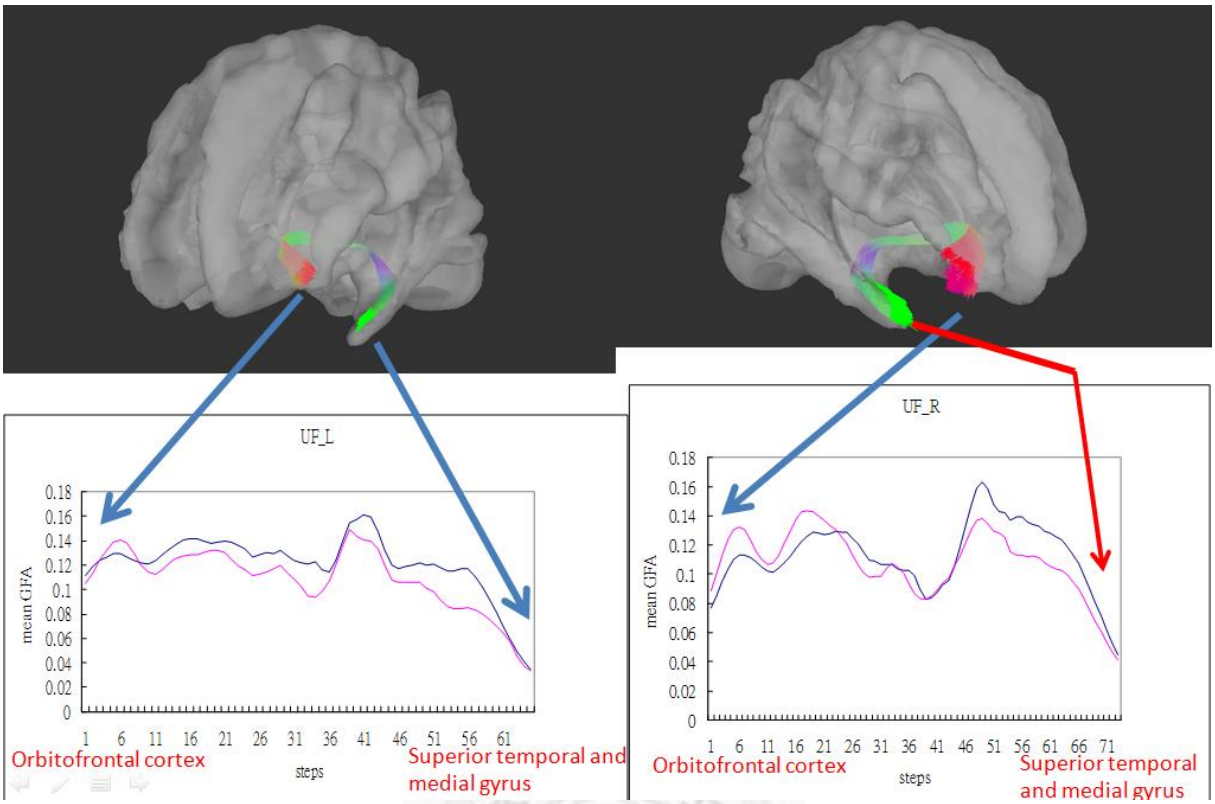

Figure 16. GFA profile of UF. In bilateral UF, we could find that the highest GFA value was existed on margin of the lateral sulcus where the UF was bending from the lateral OFC to the temporal lobe. And in left UF, the GFA values in schizophrenia were almost

lower than normal controls'. But in right UF, the GFA values in schizophrenia were higher than normal controls' in lateral OFC even throuth lower in temporal lobe as the same as left UF.

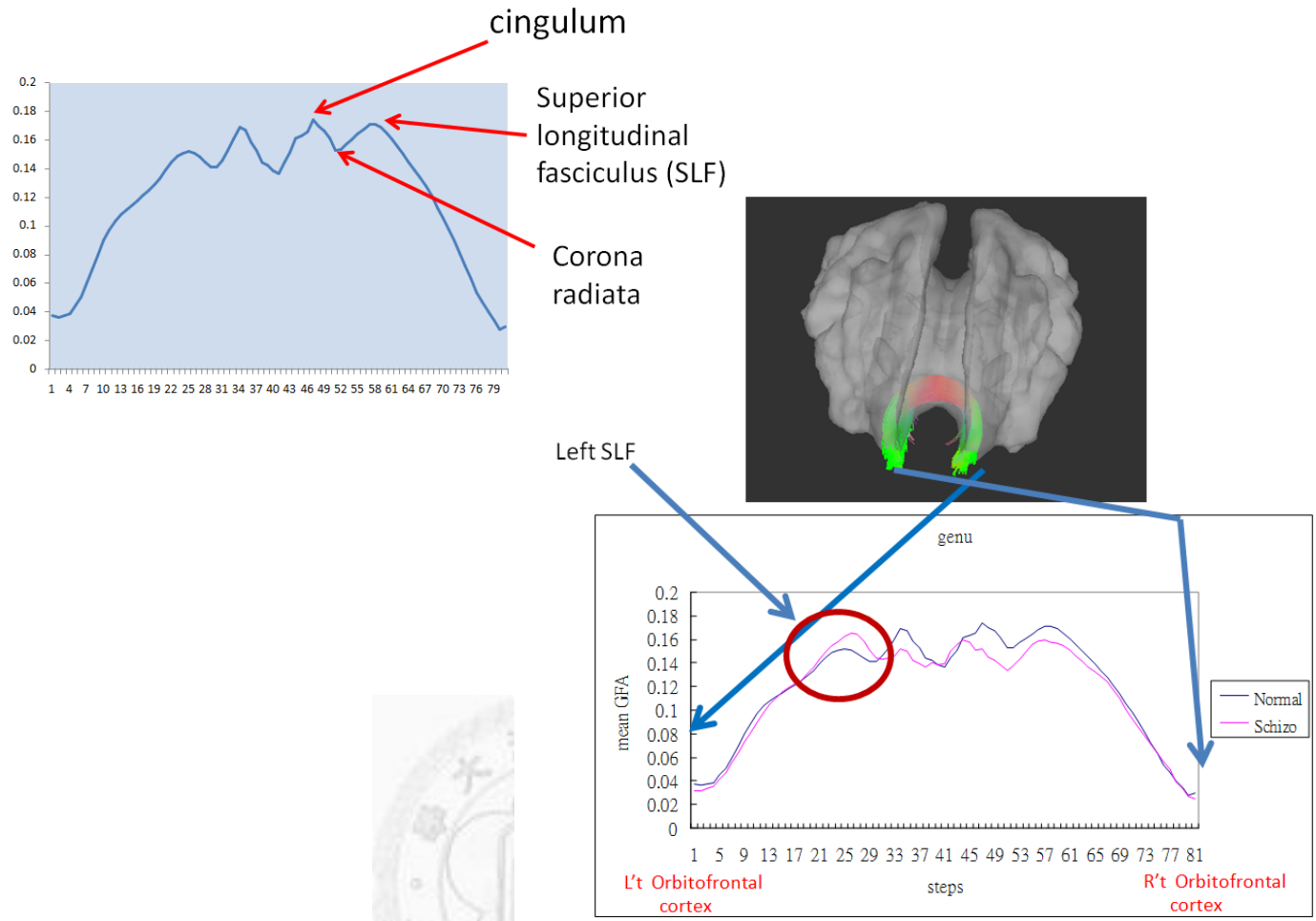

Figure 17. GFA profile of genu. The way of intersection between genu and SLF, genu and cingulm bundle was compression, and it lead the GFA values higher. However, the way of intersection between genu and coroa radiata was splicing, and it made the GFA values lower (Left). In genu, we could find that the higher GFA values was appeared on the intersection with superior longitudinal fasiculus (SLF) and cingulum bundle, and the lower GFA values was appeared on the intersection with coroa radiata (Right).

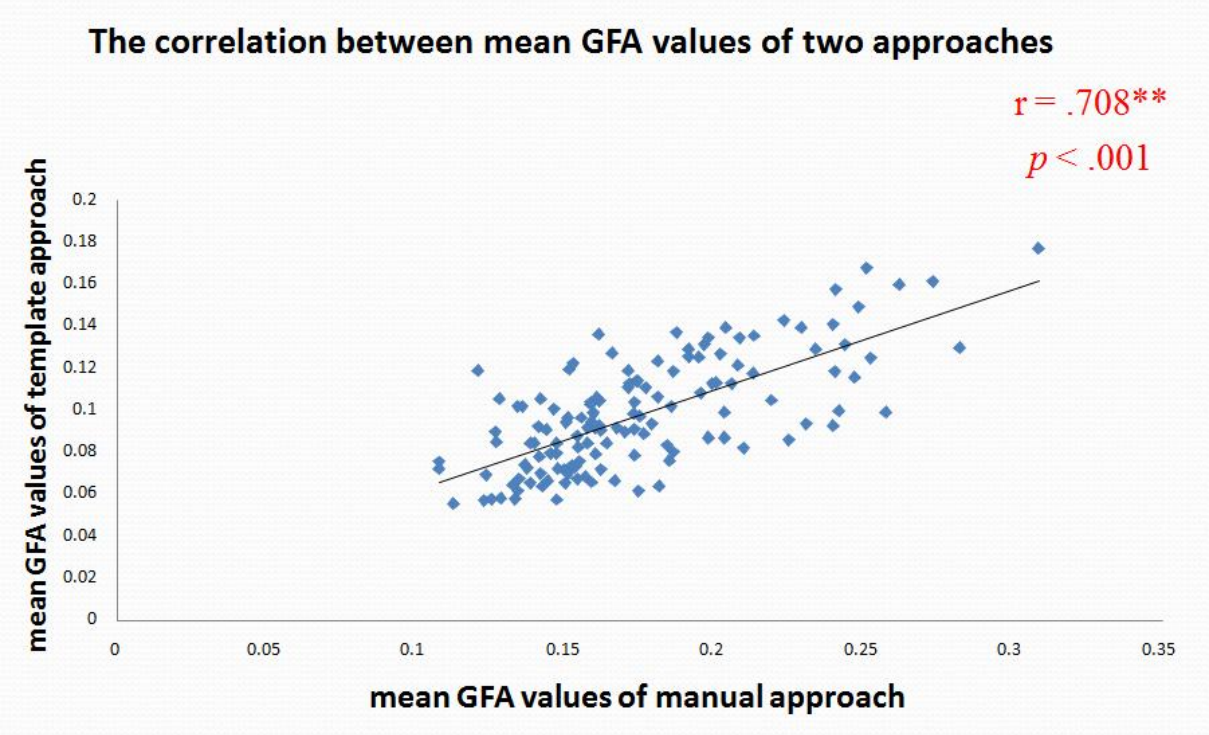

Figure 18. The correlaion of mean GFA between two approaches. There was a significant positive correlation of mean GFA values between these two approaches (r = .708**, $p < .001$).